



City Research Online

City, University of London Institutional Repository

Citation: Bittner, R., Linden, D., Roebroek, A., Haertling, F., Rotarska-Jagiela, A., Maurer, K., Goebel, R., Singer, W. & Haenschel, C. (2015). The When and Where of Working Memory Dysfunction in Early-Onset Schizophrenia-A Functional Magnetic Resonance Imaging Study. *Cerebral Cortex*, 25(9), pp. 2494-2506. doi: 10.1093/cercor/bhu050

This is the accepted version of the paper.

This version of the publication may differ from the final published version.

Permanent repository link: <https://openaccess.city.ac.uk/id/eprint/12852/>

Link to published version: <https://doi.org/10.1093/cercor/bhu050>

Copyright: City Research Online aims to make research outputs of City, University of London available to a wider audience. Copyright and Moral Rights remain with the author(s) and/or copyright holders. URLs from City Research Online may be freely distributed and linked to.

Reuse: Copies of full items can be used for personal research or study, educational, or not-for-profit purposes without prior permission or charge. Provided that the authors, title and full bibliographic details are credited, a hyperlink and/or URL is given for the original metadata page and the content is not changed in any way.

City Research Online:

<http://openaccess.city.ac.uk/>

publications@city.ac.uk

The When and Where of working memory dysfunction in early-onset schizophrenia - A functional magnetic resonance imaging study

Robert A. Bittner^{1,2,3*}, David E.J. Linden^{4,5}, Alard Roebroeck⁶, Fabian Härtling⁷, Anna Rotarska-Jagiela^{1,2}, Konrad Maurer¹, Rainer Goebel⁶, Wolf Singer^{2,3}, Corinna Haenschel^{1,8}

¹*Laboratory for Neurophysiology and Neuroimaging, Department of Psychiatry, Psychosomatic Medicine and Psychotherapy and Brain Imaging Center, University Hospital Frankfurt, Goethe University, Frankfurt am Main, Germany*

²*Department of Neurophysiology, Max-Planck-Institute for Brain Research, Frankfurt am Main, Germany*

³*Ernst Strüngmann Institute for Neuroscience (ESI) in Cooperation with Max Planck Society, Frankfurt am Main, Germany*

⁴*MRC Centre for Neuropsychiatric Genetics & Genomics, Institute of Psychological Medicine and Clinical Neurosciences, School of Medicine, Cardiff University, UK*

⁵*School of Psychology, Cardiff University, UK*

⁶*Department of Neurocognition, Faculty of Psychology and Neuroscience, Maastricht University, Maastricht, The Netherlands*

⁷*Department of Child and Adolescent Psychiatry, University Hospital Frankfurt, Goethe University, Frankfurt am Main, Germany*

⁸*School of Psychology, City University, London, UK*

*Corresponding author. Laboratory for Neurophysiology and Neuroimaging, Department of Psychiatry, Psychosomatic Medicine and Psychotherapy, University Hospital Frankfurt, Goethe University, Heinrich-Hoffmann-Str. 10, D-60528 Frankfurt am Main, Germany.

Phone: +49 69 6301 84713. Fax: +49 69 6301 87001.

Email: bittner@bic.uni-frankfurt.de

Total number of words in abstract: 200

Total number of words in text: 5638

ABSTRACT

Behavioral evidence indicates that working memory (WM) in schizophrenia is already impaired at the encoding stage. However, the neurophysiological basis of this primary deficit remains poorly understood. Using event-related fMRI we assessed differences in brain activation and functional connectivity during the encoding, maintenance and retrieval stages of a visual WM task with three levels of memory load in 17 adolescents with early-onset schizophrenia and 17 matched controls. The amount of information patients could store in WM was reduced at all memory load levels. During encoding, activation in left ventrolateral prefrontal cortex (VLPFC) and extrastriate visual cortex, which in controls positively correlated with the amount of stored information, was reduced in patients. Additionally, patients showed disturbed functional connectivity between prefrontal and visual areas. During retrieval, right inferior VLPFC hyperactivation was correlated with hypoactivation of left VLPFC in patients during encoding. Visual WM encoding is disturbed by a failure to adequately engage a visual-prefrontal network critical for the transfer of perceptual information into WM. Prefrontal hyperactivation appears to be a secondary consequence of this primary deficit. Isolating the component processes of WM can lead to more specific neurophysiological markers for translational efforts seeking to improve the treatment of cognitive dysfunction in schizophrenia.

INTRODUCTION

Working memory (WM) impairments are widely regarded as a central cognitive deficit of schizophrenia (Goldman-Rakic 1999; Silver et al. 2003). WM dysfunction has therefore gained particular interest as a target of psychological and pharmacological interventions (Green et al. 2004; Greenwood et al. 2005; Barch and Smith 2008; Barch et al. 2009) and as an intermediate phenotype in the study of the genetic architecture of schizophrenia (Meyer-Lindenberg and Weinberger 2006; Gur et al. 2007). These translational strategies critically depend upon a clear understanding of the underlying cognitive and neurophysiological disturbances.

Behavioral studies indicate that WM is primarily compromised during the initial encoding of information (Tek et al. 2002; Hartman et al. 2003; Lencz et al. 2003; Kim et al. 2006; Lee and Park 2006; Javitt et al. 2007; Fuller et al. 2009; Gold et al. 2010; Hahn et al. 2010; Mayer and Park 2012), although additional impairments during maintenance have also been observed (Reilly et al. 2006; Stephane and Pellizzer 2007; Badcock et al. 2008). Therefore, elucidating the neurophysiological basis of impaired encoding is crucial for our understanding of WM deficits. Functional magnetic resonance imaging (fMRI) studies have consistently implicated a dysfunction of the prefrontal cortex (PFC) as a central cause for WM deficits (Glahn et al. 2005; Tan et al. 2007). However, the origins of impaired encoding and the contribution of prefrontal cortical dysfunction to this impairment remain poorly understood.

In healthy participants, fMRI has provided detailed insights into the differential engagement of prefrontal areas during encoding and subsequent WM component processes. Encoding of visuospatial information appears to rely primarily on the superior part of the ventrolateral prefrontal cortex (VLPFC) (Bor et al. 2003; Mayer et

al. 2007). In contrast, for maintenance the dorsolateral prefrontal cortex (DLFPC) was shown to be crucial (Sakai et al. 2002; Curtis and D'Esposito 2003; Edin et al. 2009). Finally, the inferior portion of the VLPFC seems to be particularly important for retrieval (Bledowski et al. 2006; Nee and Jonides 2008). In line with their differential engagement, these prefrontal areas also show a corresponding preferential response to increasing memory load during the relevant component process (Linden et al. 2003; Bledowski et al. 2006; Edin et al. 2009).

These findings support a relative specialization of the PFC with regard to WM component processes. This implies that impaired encoding should be associated with disturbances in the corresponding specialized prefrontal cortical area, namely the superior part of the VLPFC. The same principle should also apply to maintenance and retrieval.

In addition to the precise localization of prefrontal cortical dysfunction, the nature of the abnormal prefrontal cortical response profile is another crucial aspect. Earlier fMRI studies reported both decreased (Barch et al. 2001; Perlstein et al. 2001; Perlstein et al. 2003) and increased prefrontal cortical activation in patients (Manoach et al. 1999; Callicott et al. 2000; Manoach et al. 2000). The latter finding has been interpreted as an indication of inefficiency (Callicott et al. 2000; Potkin et al. 2009). However, it has also been suggested that PFC dysfunction is sensitive to the level of memory load: while low memory load should elicit inefficient prefrontal hyperactivation, high memory load should lead to hypoactivation caused by a failure to sustain activation in prefrontal circuits (Callicott et al. 2003; Manoach 2003).

Yet, the use of blocked experimental designs – often in conjunction with the n-back task, has prevented the isolation of the component processes of WM in many of these studies.

So far, event-related studies were also unable to clarify the neurophysiological basis of impaired encoding. This might in part be attributable to a lack of memory load variation (Schlosser et al. 2008; Anticevic et al. 2011; Choi et al. 2011) and an incomplete separation of component processes (Johnson et al. 2006). Other event-related studies focused on predefined prefrontal regions of interest (ROIs) (Driesen et al. 2008; Potkin et al. 2009), which might obscure the precise localization of prefrontal cortical dysfunction. This approach also ignores the fact that WM – and encoding in particular – relies on a widely distributed cortical network. In addition to the PFC, WM prominently involves parietal and sensory areas (Munk et al. 2002; Linden et al. 2003), which have also been implicated in WM impairment (Barch and Csernansky 2007; Haenschel et al. 2007; Dias et al. 2011).

Such widespread cortical dysfunctions could be a reflection of disturbed interactions between brain areas as proposed by the disconnection hypothesis (Friston 1998; Andreasen 1999). This interpretation is supported by reports of altered functional connectivity during WM (Meyer-Lindenberg et al. 2005; Tan et al. 2006; Kim et al. 2009; Meda et al. 2009; Deserno et al. 2012). However, so far the role of altered functional connectivity for impaired encoding has not been investigated.

We previously reported reduced P100 event-related potential (ERP) amplitude during WM encoding in schizophrenia (Haenschel et al. 2007). In an accompanying fMRI ROI analysis (Haenschel et al. 2007) we also demonstrated a corresponding reduction of activation in those visual cortical areas most closely associated with the generation of the P100 (Noesselt et al. 2002). However, this fMRI analysis was focused on one small bilateral ROI in early visual cortex during maintenance and retrieval. While the ERP results and EEG time frequency results provided detailed insights into the temporal dynamics underlying WM dysfunction, only the high spatial

resolution of fMRI allows for a detailed study of the different parts of the cortical WM network. This aspect is particularly relevant with regard to the contribution of the distinct subregions of the PFC. To this end, in the current paper we present a full analysis of the fMRI data set.

We investigated adolescents with early-onset schizophrenia (EOS), i.e. an onset of the disorder before the age of 18, and matched controls. The study of patients with EOS is particularly attractive, because they apparently constitute a more homogeneous group characterized by a relatively severe illness course and outcome (Hollis 2000) and a higher genetic loading (Asarnow et al. 2001) compared to patients with adult onset schizophrenia. WM dysfunction in EOS has been repeatedly demonstrated. However, only a small number of functional neuroimaging studies of this patient population have been reported (Thormodsen et al. 2011; White et al. 2011a; White et al. 2011b; Kyriakopoulos et al. 2012).

Using event-related fMRI, we investigated aberrant cortical activation and connectivity during encoding and subsequent WM component processes.

Participants performed a visual delayed-discrimination task with varying levels of memory load (Figure 1). Our main hypothesis was that during encoding patients would show a dysfunction of cortical areas closely involved in this component process, particularly in the PFC. If these dysfunctional areas were crucial for encoding, we would expect them to exhibit a correlation between BOLD activity and the number of objects actually encoded and stored in WM. We also hypothesized that a primary encoding deficit should in turn lead to compensatory changes in later task phases. Finally, we expected to find abnormal functional connectivity within circuits critical for the encoding of information into WM, in line with the disconnection hypothesis of schizophrenia.

METHODS AND MATERIALS

Subjects

Seventeen patients with EOS according to DSM-IV criteria and seventeen control participants with no family history of psychotic disorder matched for age, gender, handedness and premorbid IQ (Table 1) participated in the study. ERP data (Haenschel et al. 2007), fMRI results on extrastriate visual cortex (Haenschel et al. 2007) and EEG time frequency results (Haenschel et al. 2009; Haenschel et al. 2010) obtained from the same group of patients have been reported previously. Patients were assessed with the German version of the Structured Clinical Interview for DSM-IV (SCID) (Sass and Wittchen 2003) and the Positive and Negative Syndrome Scale (PANSS) (Kay et al. 1987). Handedness was determined with the Edinburgh Handedness Inventory (Oldfield 1971). Premorbid IQ was assessed with MWT (Lehrl 1995), the German equivalent of the Spot-the-Word Test (Baddeley et al. 1993). All patients received second generation antipsychotic medication at the time of this study, with one patient additionally receiving first generation antipsychotic medication (see Table 1 for further details).

----- Table 1 -----

Exclusion criteria for patients were a history of other neuropsychiatric conditions or substance abuse in the six months preceding the study. Control participants were recruited through local advertisements. Exclusion criteria for controls were a history of mental illness or substance abuse. All participants and, for participants under 18 years, also their parents provided informed consent prior to the study. Ethical approval was obtained from the institutional review board of Frankfurt Medical School.

Stimuli and task

A delayed visual discrimination task was implemented on a personal computer using the Experimental-Run-Time-System software (www.erts.de) (Figure 1). Non-natural objects, presented at the center of the computer screen, were used as visual stimuli. One to three sample objects were presented for 600 ms each with an interstimulus interval of 400 ms (encoding phase). After a delay of 12 s (maintenance phase), a test stimulus was presented for 3 s at the center of the screen (retrieval phase). Subjects had to indicate whether it was part of the initial sample set by button press. The inter-trial interval lasted 12 s.

----- Figure 1 -----

The three memory load conditions were randomly intermixed within each run. Prior to the scanning session all participants were given instruction and practice with the task. During scanning, the computer display was projected onto a mirror mounted on the head coil. Stimuli subtended 1.34° of visual angle. Responses were registered by a custom-made fiber-optic response box. Subjects were asked to fixate upon the cross at the center of the screen throughout the experiment. Each subject completed a total of 48 trials of the task (16 trials per memory load condition).

Analysis of behavioral data

For each subject and memory load condition, the number of objects stored in WM was estimated by calculating K . We used Cowan's revised formula (Cowan 2001) $K = N * (H + CR - 1)$, where N is the number of objects to be stored, H is the observed hit rate (correctly identified matches) and CR is the correct rejection rate (correctly identified non-matches). Although originally developed to estimate overall WM storage capacity, K also allows quantifying the amount of information actually stored

in WM. K values and reaction times were entered in separate repeated-measures analyses of variance (ANOVA) to test for main effects of group (controls and patients) and memory load condition (load 1, load 2 and load 3). Significant main effects and interactions were decomposed using t-tests.

Acquisition of fMRI data

Functional MRI data were acquired with a Siemens 1.5 T Magnetom Vision MRI scanner using a gradient echo EPI sequence (16 axial slices; TR = 2000ms; TE = 60; FA = 90°, FOV = 220 x 220 mm², voxel size: 3.43 x 3.43 x 5 mm³, gap 1 mm). Slices were positioned parallel to the anterior-commissure posterior-commissure plane. Functional images were acquired in two runs in a single session, each comprising the acquisition of 350 volumes. Stimulus presentation was constantly synchronized with the fMRI sequence. Head motion was minimized with pillows. A high-resolution T1-weighted three-dimensional volume using a fast low-angle shot (T1-FLASH) sequence (voxel size: 1x1x1 mm³) was acquired for co-registration of functional data.

Functional image preprocessing

Functional data were analyzed using BrainVoyager QX 1.10.4 and the BrainVoyager QX Matlab Toolbox (www.brainvoyager.com). The first four volumes of each run were discarded to allow for T1 equilibration. Functional data preprocessing included slice scan time correction, motion correction, linear trend removal and temporal high pass filtering (high pass: 0.00867 Hz), manual alignment to the anatomical scans and transformation into Talairach coordinate space.

To minimize the impact of increased anatomical variability found in schizophrenia (Park et al. 2004), we applied a high-resolution, multiscale cortex alignment procedure, which reliably aligns corresponding gyri and sulci across subjects (Goebel et al. 2006). Anatomical scans were segmented along the white–gray matter boundary. Cortical hemispheres were reconstructed and morphed into spherical representations. Each cortical folding pattern was aligned to a dynamically updated group average through iterative morphing following a coarse-to-fine matching strategy. Based on the vertex-to-vertex referencing from the folded, topologically correct meshes to the aligned spherical representations, the functional data was mapped into a common spherical coordinate system (Fischl et al. 1999) and spatially smoothed using a nearest neighbor interpolation (FWHM 5 mm).

Analysis of intrascan motion

To assess group differences in intra-scan motion, the standard deviations for the six estimates of motion obtained during motion correction (translation in x, y, z direction and rotation around x, y, z axis) of each subject were entered into a repeated-measures ANOVA with group as the between-factor and standard deviation for the six motion estimates as the within-factor. This yielded no significant group differences ($F_{1,32}=0.47$, $p=.50$) and no significant group by motion interaction ($F_{5,160}=1.93$, $p=.15$).

Cortex-based group fMRI analysis

Multi-subject statistical analysis was performed by multiple linear regression of the BOLD signal. Only correctly answered trials were entered into our analyses. To ensure a balanced analysis, for controls a subset of correct trials equal to the number of correct trials of the patients on the respective memory load level were randomly

selected. For both groups, this resulted in a total number of 234 trials for memory load 1, 231 trials for memory load 2 and 215 trials for memory load 3 per group. For each memory load condition four task phases of interest were modeled by ideal box-car functions, which covered the first, third, fifth and eighth volume of each trial, respectively, convolved with a synthetic double-gamma hemodynamic response function. Encoding-related activity was captured by the first and retrieval-related activity by the fourth regressor. The second and third regressor reflected activity during the early and late maintenance phase. These predictors were used to build the design matrix of the experiment. We computed a voxel-wise general linear model (GLM) with a standard two-level (hierarchical) ordinary least squares fit procedure. For each task phase of interest, the obtained beta weights were entered into a random-effects level repeated-measures ANOVA with memory load condition (load 1, load 2 and load 3) as within-factor and group (controls and patients) as between-factor.

To correct for multiple comparisons, maps for the main effect of memory load, for the main effect of group and for the group by memory load interaction were first thresholded at a voxel-wise threshold of $p < .01$ (uncorrected). They were then submitted to a whole-brain correction criterion based on the estimate of the map's spatial smoothness and on an iterative procedure (Monte Carlo simulation) for estimating cluster-level false-positive rates (Forman et al. 1995; Goebel et al. 2006). During this procedure, for each simulated image (2000 iterations) all "active" clusters in the imaged volume are considered. These clusters are used to update a table reporting the counts of all clusters above this threshold for each specific size. Subsequently an alpha value is assigned to each cluster size based on its observed relative frequency during the simulations. Based on this estimation, which was

carried out separately for each map, the appropriate minimum cluster size threshold was specified in order to yield a cluster-level false-positive rate of 5%.

Task related activation

Our main goal was to detect the abnormal activation patterns underlying impaired WM in patients.

As a secondary objective, we were interested in revealing the cortical networks engaged by our WM paradigm. In this context, the main effect of memory load provides information about areas, whose activation patterns are mainly modulated by the task. However, the ANOVA approach is inherently blind to the direction of changes in the BOLD response. Therefore, the main effect of memory load cannot distinguish between areas showing task related activation and areas showing task related deactivation.

To complement our primary analysis, we computed t-tests for each memory load condition during each task phase for both groups separately utilizing the same GLM approach employed for the ANOVA. The resulting maps for each memory load condition were thresholded at an uncorrected voxel-wise threshold of $p < .01$, corrected for multiple comparisons using a cluster threshold procedure (Monte Carlo simulation, 2000 iterations) in order to yield a cluster-level false-positive rate of 5%. The results of this analysis can be found in the supplementary material (Figures S1 – S4).

Group differences

To investigate both general activation abnormalities arising independent of memory load as well as abnormal activation patterns, which are memory load dependent, we examined the results main effect of group and the group by memory load interaction

in more detail. To this end, region of interests (ROIs) were derived from each cluster showing either a significant main effect of group or a significant group by memory load interaction. For each ROI, post-hoc t-tests were performed on the extracted beta-values to test for the direction of group differences in individual memory load conditions.

Correlation between BOLD activity and the number of stored objects

To investigate the relationship between BOLD activation and the number of objects stored in WM a planned ROI based post-hoc Spearman's rank correlation between beta values and K across all three memory load conditions was computed ($\alpha = 0.00129$ (Bonferroni corrected for the total number of 39 ROIs derived from the ANOVA)).

Cortex-based functional connectivity analysis

Finally, we investigated whether impaired WM encoding is associated with a disturbance of connectivity of the PFC with other parts of the WM network. Functional connectivity was computed using the instantaneous influence term of Granger causality mapping (Roebroeck et al. 2005). As seed regions we used the only two prefrontal ROIs, which emerged from the ANOVA for encoding. Correct trials from all memory load conditions were pooled. For each subject, functional connectivity maps for both seed region were generated. Differences in functional connectivity were analyzed using t-tests (random effects level). The resulting maps were thresholded at an uncorrected voxel-wise threshold of $p < .01$, corrected for multiple comparisons using a cluster threshold procedure (Monte Carlo simulation, 2000 iterations) in order to yield a cluster-level false-positive rate of 5%.

RESULTS:

Behavioral Performance

Figure 2 depicts the estimated number of objects stored in WM (K) and average response times for patients and controls. K was lower for patients ($F_{(1,32)}=14.31$, $p<0.001$), with no interaction between group and memory load ($F_{(2,64)}=2.46$, $p=0.093$). Two-tailed t-tests showed that the number of stored objects was lower in patients in each memory load condition (memory load 1: $t=2.65$, $p<0.05$; memory load 2: $t=3.76$, $p<0.001$; memory load 3: $t=2.39$, $p<0.05$). Reaction times increased with memory load in both groups ($F_{(2,64)}=23.26$, $p<0.001$). There was no difference in reaction times between groups ($F_{(1,32)}=2.49$, $p=0.12$) and no memory load by group interaction ($F_{(2,64)}=0.26$, $p=0.95$).

----- Figure 2 -----

ANOVA

Task related activity

The main effect of WM load demonstrated a differential effect of WM load on cortical activation during the different task phases. The effect of increasing levels of WM load was most pronounced during encoding and the initial part of the maintenance phase. Conversely, the degree to which WM load was driving activation markedly decreased during the later stages of the delay period and particularly during retrieval. This finding is in keeping with previous studies utilizing the same task (Linden et al. 2003; Bledowski et al. 2006). These studies revealed widespread cortical activation during the maintenance and retrieval stages. However, compared to encoding this activation was far less modulated by WM load. Thus, relying only on the main effect of memory load would underestimate the full extent of task related activation.

The additional t-statistics (Figure S1-S4) revealed considerable task related activation in a distributed network comprising frontal, parietal and visual areas commonly observed in studies of visual WM (Munk et al. 2002). During the maintenance phase, a core fronto-parietal network showed persistent activity. Furthermore, we observed task related deactivation in the default mode network (DMN) well in line with previous WM studies (Mayer et al. 2010).

Group differences

For our main goal, the identification of abnormal activation in patients, we focused on areas showing a main effect of group or a group by memory load interaction. Beta-values of these ROIs for each task phase are depicted in the supplementary material (Figures S5-S8).

For *encoding*, the ANOVA yielded a main effect of group in the left VLPFC and left inferior parietal lobule (IPL) (cluster level threshold (CLT) 37 mm²) (Figure 3a, Table 2). Post-hoc t-tests indicated reduced activation for patients in both regions for all three memory load conditions.

A group by memory load interaction was observed in the left VLPFC caudally of the region showing a main effect of group, the left insula, left middle temporal gyrus (MTG), left precuneus, the right IPL and right lingual gyrus (CLT 52 mm²). Post-hoc t-tests indicated reduced activation for patients in the left VLPFC and the left MTG at memory load 2 and 3. In the left precuneus patients showed reduced activation only at memory load 3. In the left insula, the right IPL and the right lingual gyrus a pattern compatible with a memory load dependent dysfunction was found. Here, patients showed increased activation at memory load 1 but reduced activation at memory load

3. Finally, in the right lingual gyrus patients showed reduced activation at memory load 2.

----- Figure 3 -----

----- Table 2 -----

For *early maintenance*, the ANOVA yielded a main effect of group in the following areas: the posterior cingulate cortex (PCC), precuneus and middle occipital gyrus (MOG) bilaterally, the left insula and left MTG, the right central sulcus, right supramarginal gyrus (SMG), right superior temporal gyrus (STG) and right lingual gyrus (CLT 61 mm²) (Figure 4, Table 3). Post-hoc t-tests indicated reduced activation for patients in each of these regions for all three memory load conditions.

A group by memory load interaction was observed in the superior parietal lobule (SPL) bilaterally, the left DLPFC, the left frontal eye field (FEF), and two clusters in the left intraparietal sulcus (IPS) (CLT 33 mm²). Post-hoc t-tests indicated reduced activation for patients in the left DLPFC, the right SPL and both clusters in the left IPS at memory load 3. In the more lateral left IPS cluster, patients showed increased activation at memory load 2. Similarly, in the left DLPFC patients showed a trend towards increased activation ($p=0.056$) at memory load 1.

----- Figure 4 -----

----- Table 3 -----

For *late maintenance*, the ANOVA yielded a main effect of group in three regions (CLT 37 mm²) (Figure 5a, Table 4). In the left STG and the left PCC activation patients showed decreased activation at memory load 2 and 3. This was due to a

deactivation in patients, which increased with increasing memory load and was absent in controls. Conversely, in the left FEF patients showed increased activation in all memory load conditions. No area showed a group by memory load interaction.

----- Figure 5 -----

----- Table 4 -----

For *retrieval*, the ANOVA yielded a main effect of group in the anterior cingulate cortex (ACC), inferior VLPFC and IPL bilaterally as well as in the left anterior PFC (CLT 15 mm²) (Figure 6, Table 5). Post-hoc t-tests indicated higher activation for patients in each of these regions at memory load 2 and 3. This effect extended to memory load 1 in the IPL bilaterally.

A memory load by group interaction was observed in the left fusiform gyrus (FFG) and the right ACC (CLT 37 mm²). Post-hoc t-tests indicated higher activation in controls in the left FFG at memory load 1. In the right ACC controls showed higher activation at memory load 1, while patients showed higher activation at memory load 2.

----- Figure 6 -----

----- Table 5 -----

Correlation between BOLD activity and the number of stored objects

During encoding controls but not patients showed a significant positive correlation between BOLD activity and the number of objects stored in WM for the left posterior VLPFC ($\rho = 0.445$, $p < .05$, corr.), the left insula ($\rho = 0.549$, $p < .01$, corr.) and the right lingual gyrus ($\rho = 0.44725$, $p < .05$, corr.) (Figure 3b). In contrast, during late maintenance patients but not controls showed a significant negative correlation

between BOLD activity and the number of objects stored in WM in the left STG ($\rho = -0.603$, $p < .001$, corr.) and the left PCC ($\rho = -0.543$, $p < .01$, corr.) (Figure 5b). During early maintenance and retrieval no significant correlation was observed in either group.

For the two ROIs for which patients showed a significant negative correlation between BOLD activity and K, we aimed to specify whether these disparate results could be explained by a general difference in BOLD activity or by differences in K. To this end, we carried out an additional post-hoc ANCOVA with BOLD activity as within-factor, group (controls and patients) as between-factor and K as a covariate. A significant effect of group was observed in both the left STG ($F(1,99) = 17.16$, $p < 0.001$) and the left PCC ($F(1,99) = 15.84$, $p < 0.001$). This indicates that these findings may primarily be the result of differences in BOLD activity between patients and controls.

Correlation of activation across task phase

We also examined whether prefrontal hypoactivation in patients during encoding might be correlated with prefrontal hyperactivation during retrieval. Such a correlation would strengthen our hypothesis of a primary encoding deficit. In the previous analysis, we found a correlation between BOLD activity and the number of objects stored in WM (K) in parts of the left prefrontal cortex during encoding. However this correlation was only observed in controls. To minimize any bias resulting from a potential differential relationship between BOLD activity and K in patients and controls, we conducted post-hoc partial correlations, which controlled for K. These partial correlations were computed between the two left hemispheric VLPFC clusters,

for which patients showed hypoactivation during encoding, and the bilateral clusters in inferior VLPFC, for which patients showed hyperactivation during retrieval. A correlation across component processes was observed in both groups between the left posterior VLPFC cluster from the encoding map and the right inferior VLPFC cluster from the retrieval map. However, while patients showed a negative correlation ($\rho=-0.361$, $p=.01$) controls showed a positive correlation ($\rho=0.326$, $p<.05$).

Functional connectivity analysis

Significant differences in functional connectivity between groups were found in one of the two tested prefrontal seed regions, namely the more rostral left VLPFC cluster. For this region, patients showed reduced functional coupling with the left precentral gyrus (PCG) (Talairach coordinates x: -45, y: -6, z: 43) corresponding to the premotor cortex and an area in the left MOG (Talairach coordinates x: -44, y: -60, z: -4) corresponding to the lateral occipital complex (LOC) (Malach et al. 1995) (CLT 45 mm²) (Figure 7). For the second seed region, the more dorsal left VLPFC cluster no significant group differences in functional connectivity emerged.

----- Figure 7 -----

DISCUSSION

We investigated the neurophysiological basis of impaired WM encoding in adolescents with schizophrenia compared to healthy controls performing a visual WM task with three levels of memory load. At all memory load levels, the amount of information patients were able to memorize was reduced compared to controls. Patients exhibited abnormal activity patterns in key regions of the fronto-parietal network and in extrastriate visual areas, which were specific for the different WM component processes. Impaired encoding in patients was also accompanied by disturbed functional connectivity between prefrontal and visual areas.

Patterns of cortical dysfunction during encoding in patients were largely indicative of a general impairment of this component process. Patients showed hypoactivation, particularly at higher memory load, in two overlapping clusters within a part of the left VLPFC closely linked to WM encoding (Bor et al. 2003; Mayer et al. 2007). This confirms our initial hypothesis, that impaired encoding is associated with a dysfunction in those prefrontal areas most specialized for this component process. Patients also failed to recruit the left IPL, which is closely involved in encoding as well (Linden et al. 2003; Mayer et al. 2007).

During encoding, only controls showed a significant positive correlation between the amount of information stored in WM and BOLD activity in the left VLPFC, insula and extrastriate visual cortex. These areas also showed generally lower activation levels in patients. Thus, impaired encoding in patients appears to result from a dysfunction of both prefrontal and visual areas critical for this component process.

Further support for this interpretation comes from our functional connectivity analysis. During encoding, patients showed significantly reduced functional connectivity

between the left VLPFC and the left premotor cortex as well as the left LOC. The latter areas is essential for the detailed processing of object information (Grill-Spector et al. 1998).

These findings extend our previous reports of abnormal ERP (Haenschel et al. 2007) and evoked oscillatory responses (Haenschel et al. 2009) during encoding in the same group of patients. They indicate that in addition to disturbances at early stages of visual processing impaired encoding is associated with a disruption of communication between the ventral visual pathway and the VLPFC (Ungerleider et al. 1998). Thus, mechanisms critical for object recognition (Sehatpour et al. 2008) and object WM (Goldman-Rakic 1995) seem to be affected. Our results are compatible with the view that perceptual processing deficits contribute to WM impairment (Haenschel et al. 2007; Koychev et al. 2010; Dias et al. 2011). They also indicate a link between perturbed perceptual processing and prefrontal cortical dysfunction. However, due to the lack of directional information the analysis of functional connectivity cannot resolve the question, whether either one of them or both represent a primary deficit.

Moreover, WM encoding can be further subdivided into a number of cognitive processes including WM consolidation (Jolicoeur and Dell'Acqua 1998) and attentional selection (Awh et al. 2006). Behavioral studies indicate that patients with schizophrenia are impaired in these processes (Luck and Gold 2008; Fuller et al. 2009; Hahn et al. 2010). The neurophysiological underpinnings of these impairments and their exact contribution to disturbed WM encoding need to be elucidated in future studies.

While our primary goal was to clarify the neurophysiological substrate of impaired encoding, two findings during the subsequent component processes are also

particularly relevant to neuropsychological and neurophysiological models of schizophrenia. During early maintenance, patients showed an abnormally strong deactivation in parts of the default mode network (DMN) (Raichle et al. 2001) including bilateral PCC and precuneus. During late maintenance, the left STG and the left PCC exhibited a similar pattern. Here, only patients showed a negative correlation between BOLD activity and the number of objects stored in WM. Thus, deactivation in parts of the DMN was stronger in patients with a relatively preserved ability to store information in WM. Whether this indicates a compensatory mechanism in patients which supports WM maintenance or whether a failure to adequately disengage the DMN actually impairs WM cannot be determined on the basis of the present results. However, the observed correlation between BOLD activity and performance in patients point to a particular relevance of this network for WM dysfunction. Furthermore, our results are in line with increasing evidence for alterations within the DMN in schizophrenia (Whitfield-Gabrieli et al. 2009; Metzak et al. 2011).

During retrieval, patients showed a marked hyperactivation at all memory load levels in a bilateral network encompassing the inferior VLPFC, ACC, and IPL. These areas are essential for WM retrieval (Druzgal and D'Esposito 2001; Bledowski et al. 2006; Nee and Jonides 2008). Their increased recruitment could reflect an inefficient engagement of WM read out mechanisms in patients, which might result from their relatively imprecise memory representations. Such an interpretation is also supported by the negative correlation between BOLD activity in the left VLPFC during encoding with that in the right inferior VLPFC during retrieval in patients. Thus, prefrontal inefficiency during retrieval was more prominent in those patients who showed more PFC hypoactivation during the initial encoding of information.

Our findings have implications for our understanding of WM related prefrontal cortical dysfunction in schizophrenia. Prefrontal inefficiency, indexed by hyperactivation, is regarded as an important marker of this dysfunction (Winterer and Weinberger 2004). However, in the present study it was only observed during retrieval. Consequently, prefrontal inefficiency could constitute a secondary phenomenon, while prefrontal hypoactivation associated with abnormal encoding might be the primary manifestation of prefrontal cortical dysfunction. Notably, the prefrontal hyperactivation observed in a large, multisite patient cohort was also associated with retrieval (Potkin et al. 2009). We found no indication of a memory load dependent prefrontal cortical dysfunction (Callicott et al. 2003; Manoach 2003) during encoding. Such a switch from hyperactivation at low memory load to hypoactivation at high memory load was only observed in the left DLPFC during early maintenance. However, the fact that this prefrontal response profile occurred after the initial prefrontal hypoactivation during encoding indicates, that it might not represent a primary deficit. Overall, our findings imply that prefrontal cortical dysfunction is more sensitive to the demands of a particular WM component process than to the level of memory load. The fact, that we observed abnormal prefrontal activation in those parts of the PFC shown to be particularly relevant for each WM component process, also supports such an interpretation.

Interestingly, a recent fMRI study using a visuospatial WM paradigm did not find abnormal prefrontal cortical activation in patients with EOS (White et al. 2011a). Notably, on average their patient group was about 3 years younger than ours while having a similar duration of illness. Based on their negative finding White and colleagues hypothesized, that prefrontal cortical dysfunction might be the result of a downstream developmental process, which had not yet manifested itself in their

patient group. In contrast, our finding of a robust prefrontal cortical dysfunction is well in line with findings in patients with adult-onset schizophrenia.

In summary, the primary impairment of WM encoding seems to arise from disturbances in both early visual and prefrontal areas and a disruption of neuronal communication between these areas in line with the disconnection hypothesis of schizophrenia. Isolating the component processes of WM allowed us to better differentiate between primary and secondary markers of cortical dysfunction. This might be crucial for the development of reliable biological markers (Oertel-Knoechel et al. 2011; Barch et al. 2012; Linden 2012) and pharmacological compounds targeting WM dysfunction (Barch 2004). Therefore, our approach should aid translational studies, which probe the pathways from the molecular mechanisms to the phenotypes of schizophrenia (Meyer-Lindenberg 2010).

Acknowledgements

The authors are grateful to Tanya Goncharova, Marcus Cap, and Steffen Konz for help with data acquisition, to Jochen Weber for the implementation of additional analysis algorithms in the BrainVoyager QX Matlab Toolbox, and to Jutta S. Mayer and Armin Heinecke for helpful discussions. Robert A. Bittner takes responsibility for the integrity of the data and the accuracy of the data analyses. All authors had full access to all of the data in the study. This study was supported by the Max Planck Society and by grant BMBF 01 GO 0508 from the German Ministry of Education.

Disclosure of biomedical financial interests and potential conflicts of interest

All authors report no biomedical financial interests or potential conflicts of interest.

REFERENCES

- Andreasen NC. 1999. A unitary model of schizophrenia: Bleuler's "fragmented phrene" as schizencephaly. *Arch Gen Psychiatry* 56:781-787.
- Anticevic A, Repovs G, Barch DM. 2011. Working Memory Encoding and Maintenance Deficits in Schizophrenia: Neural Evidence for Activation and Deactivation Abnormalities. *Schizophrenia bulletin*.
- Asarnow RF, Nuechterlein KH, Fogelson D, Subotnik KL, Payne DA, Russell AT, Asamen J, Kuppinger H, Kendler KS. 2001. Schizophrenia and schizophrenia-spectrum personality disorders in the first-degree relatives of children with schizophrenia: the UCLA family study. *Arch Gen Psychiatry* 58:581-588.
- Awh E, Vogel EK, Oh SH. 2006. Interactions between attention and working memory. *Neuroscience* 139:201-208.
- Badcock JC, Badcock DR, Read C, Jablensky A. 2008. Examining encoding imprecision in spatial working memory in schizophrenia. *Schizophrenia research* 100:144-152.
- Baddeley A, Emslie H, Nimmo-Smith I. 1993. The Spot-the-Word test: a robust estimate of verbal intelligence based on lexical decision. *The British journal of clinical psychology / the British Psychological Society* 32 (Pt 1):55-65.
- Barch DM. 2004. Pharmacological manipulation of human working memory. *Psychopharmacology (Berl)* 174:126-135.
- Barch DM, Berman MG, Engle R, Jones JH, Jonides J, Macdonald A, 3rd, Nee DE, Redick TS, Sponheim SR. 2009. CNTRICS final task selection: working memory. *Schizophrenia bulletin* 35:136-152.
- Barch DM, Carter CS, Braver TS, Sabb FW, MacDonald A, 3rd, Noll DC, Cohen JD. 2001. Selective deficits in prefrontal cortex function in medication-naïve patients with schizophrenia. *Arch Gen Psychiatry* 58:280-288.
- Barch DM, Csernansky JG. 2007. Abnormal parietal cortex activation during working memory in schizophrenia: verbal phonological coding disturbances versus domain-general executive dysfunction. *Am J Psychiatry* 164:1090-1098.
- Barch DM, Moore H, Nee DE, Manoach DS, Luck SJ. 2012. CNTRICS Imaging Biomarkers Selection: Working Memory. *Schizophrenia bulletin* 38:43-52.
- Barch DM, Smith E. 2008. The cognitive neuroscience of working memory: relevance to CNTRICS and schizophrenia. *Biological psychiatry* 64:11-17.
- Bledowski C, Cohen Kadosh K, Wibrall M, Rahm B, Bittner RA, Hoechstetter K, Scherg M, Maurer K, Goebel R, Linden DE. 2006. Mental chronometry of working memory retrieval: a combined functional magnetic resonance imaging and event-related potentials approach. *J Neurosci* 26:821-829.
- Bor D, Duncan J, Wiseman RJ, Owen AM. 2003. Encoding strategies dissociate prefrontal activity from working memory demand. *Neuron* 37:361-367.
- Callicott JH, Bertolino A, Mattay VS, Langheim FJ, Duyn J, Coppola R, Goldberg TE, Weinberger DR. 2000. Physiological dysfunction of the dorsolateral prefrontal cortex in schizophrenia revisited. *Cereb Cortex* 10:1078-1092.
- Callicott JH, Mattay VS, Verchinski BA, Marenco S, Egan MF, Weinberger DR. 2003. Complexity of prefrontal cortical dysfunction in schizophrenia: more than up or down. *Am J Psychiatry* 160:2209-2215.
- Choi JS, Park JY, Jung MH, Jang JH, Kang DH, Jung WH, Han JY, Choi CH, Hong KS, Kwon JS. 2011. Phase-Specific Brain Change of Spatial Working Memory Processing in Genetic and Ultra-High Risk Groups of Schizophrenia. *Schizophrenia bulletin*.
- Cowan N. 2001. The magical number 4 in short-term memory: a reconsideration of mental storage capacity. *The Behavioral and brain sciences* 24:87-114; discussion 114-185.
- Curtis CE, D'Esposito M. 2003. Persistent activity in the prefrontal cortex during working memory. *Trends in cognitive sciences* 7:415-423.
- Deserno L, Sterzer P, Wustenberg T, Heinz A, Schlagenhaut F. 2012. Reduced prefrontal-parietal effective connectivity and working memory deficits in schizophrenia. *J Neurosci* 32:12-20.

- Dias EC, Butler PD, Hoptman MJ, Javitt DC. 2011. Early sensory contributions to contextual encoding deficits in schizophrenia. *Arch Gen Psychiatry* 68:654-664.
- Driesen NR, Leung HC, Calhoun VD, Constable RT, Gueorguieva R, Hoffman R, Skudlarski P, Goldman-Rakic PS, Krystal JH. 2008. Impairment of Working Memory Maintenance and Response in Schizophrenia: Functional Magnetic Resonance Imaging Evidence. *Biological psychiatry*.
- Druzgal TJ, D'Esposito M. 2001. A neural network reflecting decisions about human faces. *Neuron* 32:947-955.
- Edin F, Klingberg T, Johansson P, McNab F, Tegner J, Compte A. 2009. Mechanism for top-down control of working memory capacity. *Proceedings of the National Academy of Sciences of the United States of America* 106:6802-6807.
- Fischl B, Sereno MI, Dale AM. 1999. Cortical surface-based analysis. II: Inflation, flattening, and a surface-based coordinate system. *NeuroImage* 9:195-207.
- Forman SD, Cohen JD, Fitzgerald M, Eddy WF, Mintun MA, Noll DC. 1995. Improved assessment of significant activation in functional magnetic resonance imaging (fMRI): use of a cluster-size threshold. *Magn Reson Med* 33:636-647.
- Friston KJ. 1998. The disconnection hypothesis. *Schizophrenia research* 30:115-125.
- Fuller RL, Luck SJ, Braun EL, Robinson BM, McMahon RP, Gold JM. 2009. Impaired visual working memory consolidation in schizophrenia. *Neuropsychology* 23:71-80.
- Glahn DC, Ragland JD, Abramoff A, Barrett J, Laird AR, Bearden CE, Velligan DI. 2005. Beyond hypofrontality: a quantitative meta-analysis of functional neuroimaging studies of working memory in schizophrenia. *Human brain mapping* 25:60-69.
- Goebel R, Esposito F, Formisano E. 2006. Analysis of functional image analysis contest (FIAC) data with brainvoyager QX: From single-subject to cortically aligned group general linear model analysis and self-organizing group independent component analysis. *Human brain mapping* 27:392-401.
- Gold JM, Hahn B, Zhang WW, Robinson BM, Kappenman ES, Beck VM, Luck SJ. 2010. Reduced capacity but spared precision and maintenance of working memory representations in schizophrenia. *Arch Gen Psychiatry* 67:570-577.
- Goldman-Rakic PS. 1995. Architecture of the prefrontal cortex and the central executive. *Annals of the New York Academy of Sciences* 769:71-83.
- Goldman-Rakic PS. 1999. The physiological approach: functional architecture of working memory and disordered cognition in schizophrenia. *Biological psychiatry* 46:650-661.
- Green MF, Nuechterlein KH, Gold JM, Barch DM, Cohen J, Essock S, Fenton WS, Frese F, Goldberg TE, Heaton RK, Keefe RS, Kern RS, Kraemer H, Stover E, Weinberger DR, Zalcman S, Marder SR. 2004. Approaching a consensus cognitive battery for clinical trials in schizophrenia: the NIMH-MATRICES conference to select cognitive domains and test criteria. *Biological psychiatry* 56:301-307.
- Greenwood KE, Landau S, Wykes T. 2005. Negative symptoms and specific cognitive impairments as combined targets for improved functional outcome within cognitive remediation therapy. *Schizophrenia bulletin* 31:910-921.
- Grill-Spector K, Kushnir T, Edelman S, Itzchak Y, Malach R. 1998. Cue-invariant activation in object-related areas of the human occipital lobe. *Neuron* 21:191-202.
- Gur RE, Calkins ME, Gur RC, Horan WP, Nuechterlein KH, Seidman LJ, Stone WS. 2007. The Consortium on the Genetics of Schizophrenia: neurocognitive endophenotypes. *Schizophrenia bulletin* 33:49-68.
- Haenschel C, Bittner RA, Haertling F, Rotarska-Jagiela A, Maurer K, Singer W, Linden DE. 2007. Contribution of impaired early-stage visual processing to working memory dysfunction in adolescents with schizophrenia: a study with event-related potentials and functional magnetic resonance imaging. *Arch Gen Psychiatry* 64:1229-1240.
- Haenschel C, Bittner RA, Waltz J, Haertling F, Wibrall M, Singer W, Linden DE, Rodriguez E. 2009. Cortical oscillatory activity is critical for working memory as revealed by deficits in early-onset schizophrenia. *J Neurosci* 29:9481-9489.
- Haenschel C, Linden DE, Bittner RA, Singer W, Hanslmayr S. 2010. Alpha phase locking predicts residual working memory performance in schizophrenia. *Biological psychiatry* 68:595-598.

- Hahn B, Robinson BM, Kaiser ST, Harvey AN, Beck VM, Leonard CJ, Kappenman ES, Luck SJ, Gold JM. 2010. Failure of schizophrenia patients to overcome salient distractors during working memory encoding. *Biological psychiatry* 68:603-609.
- Hartman M, Steketee MC, Silva S, Lanning K, McCann H. 2003. Working memory and schizophrenia: evidence for slowed encoding. *Schizophrenia research* 59:99-113.
- Hollis C. 2000. Adult outcomes of child- and adolescent-onset schizophrenia: diagnostic stability and predictive validity. *Am J Psychiatry* 157:1652-1659.
- Javitt DC, Rabinowicz E, Silipo G, Dias EC. 2007. Encoding vs. retention: differential effects of cue manipulation on working memory performance in schizophrenia. *Schizophrenia research* 91:159-168.
- Johnson MR, Morris NA, Astur RS, Calhoun VD, Mathalon DH, Kiehl KA, Pearlson GD. 2006. A functional magnetic resonance imaging study of working memory abnormalities in schizophrenia. *Biological psychiatry* 60:11-21.
- Jolicoeur P, Dell'Acqua R. 1998. The demonstration of short-term consolidation. *Cognitive psychology* 36:138-202.
- Kay SR, Fiszbein A, Opler LA. 1987. The positive and negative syndrome scale (PANSS) for schizophrenia. *Schizophrenia bulletin* 13:261-276.
- Kim DI, Manoach DS, Mathalon DH, Turner JA, Mannell M, Brown GG, Ford JM, Gollub RL, White T, Wible C, Belger A, Bockholt HJ, Clark VP, Lauriello J, O'Leary D, Mueller BA, Lim KO, Andreasen N, Potkin SG, Calhoun VD. 2009. Dysregulation of working memory and default-mode networks in schizophrenia using independent component analysis, an fBIRN and MCIC study. *Human brain mapping*.
- Kim J, Park S, Shin YW, Jin Lee K, Kwon JS. 2006. Self-initiated encoding facilitates object working memory in schizophrenia: implications for the etiology of working memory deficit. *Schizophrenia research* 82:65-74.
- Koychev I, El-Deredy W, Haenschel C, Deakin JF. 2010. Visual information processing deficits as biomarkers of vulnerability to schizophrenia: An event-related potential study in schizotypy. *Neuropsychologia*.
- Kyriakopoulos M, Dima D, Roiser JP, Corrigall R, Barker GJ, Frangou S. 2012. Abnormal functional activation and connectivity in the working memory network in early-onset schizophrenia. *Journal of the American Academy of Child and Adolescent Psychiatry* 51:911-920 e912.
- Lee J, Park S. 2006. The role of stimulus salience in CPT-AX performance of schizophrenia patients. *Schizophrenia research* 81:191-197.
- Lehrl S. 1995. Mehrfachwahl-Wortschatz-Intelligenztest. MWT-B. Erlangen: Straube.
- Lencz T, Bilder RM, Turkel E, Goldman RS, Robinson D, Kane JM, Lieberman JA. 2003. Impairments in perceptual competency and maintenance on a visual delayed match-to-sample test in first-episode schizophrenia. *Arch Gen Psychiatry* 60:238-243.
- Linden DE. 2012. The challenges and promise of neuroimaging in psychiatry. *Neuron* 73:8-22.
- Linden DE, Bittner RA, Muckli L, Waltz JA, Kriegeskorte N, Goebel R, Singer W, Munk MH. 2003. Cortical capacity constraints for visual working memory: dissociation of fMRI load effects in a fronto-parietal network. *NeuroImage* 20:1518-1530.
- Luck SJ, Gold JM. 2008. The construct of attention in schizophrenia. *Biological psychiatry* 64:34-39.
- Malach R, Reppas JB, Benson RR, Kwong KK, Jiang H, Kennedy WA, Ledden PJ, Brady TJ, Rosen BR, Tootell RB. 1995. Object-related activity revealed by functional magnetic resonance imaging in human occipital cortex. *Proceedings of the National Academy of Sciences of the United States of America* 92:8135-8139.
- Manoach DS. 2003. Prefrontal cortex dysfunction during working memory performance in schizophrenia: reconciling discrepant findings. *Schizophrenia research* 60:285-298.
- Manoach DS, Gollub RL, Benson ES, Searl MM, Goff DC, Halpern E, Saper CB, Rauch SL. 2000. Schizophrenic subjects show aberrant fMRI activation of dorsolateral prefrontal cortex and basal ganglia during working memory performance. *Biological psychiatry* 48:99-109.
- Manoach DS, Press DZ, Thangaraj V, Searl MM, Goff DC, Halpern E, Saper CB, Warach S. 1999. Schizophrenic subjects activate dorsolateral prefrontal cortex during a working memory task, as measured by fMRI. *Biological psychiatry* 45:1128-1137.

- Mayer JS, Bittner RA, Nikolic D, Bledowski C, Goebel R, Linden DE. 2007. Common neural substrates for visual working memory and attention. *NeuroImage* 36:441-453.
- Mayer JS, Park S. 2012. Working Memory Encoding and False Memory in Schizophrenia and Bipolar Disorder in a Spatial Delayed Response Task. *J Abnorm Psychol*.
- Mayer JS, Roebroek A, Maurer K, Linden DE. 2010. Specialization in the default mode: Task-induced brain deactivations dissociate between visual working memory and attention. *Human brain mapping* 31:126-139.
- Meda SA, Stevens MC, Folley BS, Calhoun VD, Pearlson GD. 2009. Evidence for anomalous network connectivity during working memory encoding in schizophrenia: an ICA based analysis. *PLoS one* 4:e7911.
- Metzak PD, Riley JD, Wang L, Whitman JC, Ngan ET, Woodward TS. 2011. Decreased Efficiency of Task-Positive and Task-Negative Networks During Working Memory in Schizophrenia. *Schizophrenia bulletin*.
- Meyer-Lindenberg A. 2010. From maps to mechanisms through neuroimaging of schizophrenia. *Nature* 468:194-202.
- Meyer-Lindenberg A, Weinberger DR. 2006. Intermediate phenotypes and genetic mechanisms of psychiatric disorders. *Nature reviews* 7:818-827.
- Meyer-Lindenberg AS, Olsen RK, Kohn PD, Brown T, Egan MF, Weinberger DR, Berman KF. 2005. Regionally specific disturbance of dorsolateral prefrontal-hippocampal functional connectivity in schizophrenia. *Arch Gen Psychiatry* 62:379-386.
- Munk MH, Linden DE, Muckli L, Lanfermann H, Zanella FE, Singer W, Goebel R. 2002. Distributed cortical systems in visual short-term memory revealed by event-related functional magnetic resonance imaging. *Cereb Cortex* 12:866-876.
- Nee DE, Jonides J. 2008. Neural correlates of access to short-term memory. *Proceedings of the National Academy of Sciences of the United States of America* 105:14228-14233.
- Noesselt T, Hillyard SA, Woldorff MG, Schoenfeld A, Hagner T, Jancke L, Tempelmann C, Hinrichs H, Heinze HJ. 2002. Delayed striate cortical activation during spatial attention. *Neuron* 35:575-587.
- Oertel-Knoechel V, Bittner RA, Knoechel C, Prvulovic D, Hampel H. 2011. Discovery and development of integrative biological markers for schizophrenia. *Progress in neurobiology* 95:686-702.
- Oldfield RC. 1971. The assessment and analysis of handedness: the Edinburgh inventory. *Neuropsychologia* 9:97-113.
- Park HJ, Levitt J, Shenton ME, Salisbury DF, Kubicki M, Kikinis R, Jolesz FA, McCarley RW. 2004. An MRI study of spatial probability brain map differences between first-episode schizophrenia and normal controls. *NeuroImage* 22:1231-1246.
- Perlstein WM, Carter CS, Noll DC, Cohen JD. 2001. Relation of prefrontal cortex dysfunction to working memory and symptoms in schizophrenia. *Am J Psychiatry* 158:1105-1113.
- Perlstein WM, Dixit NK, Carter CS, Noll DC, Cohen JD. 2003. Prefrontal cortex dysfunction mediates deficits in working memory and prepotent responding in schizophrenia. *Biological psychiatry* 53:25-38.
- Potkin SG, Turner JA, Brown GG, McCarthy G, Greve DN, Glover GH, Manoach DS, Belger A, Diaz M, Wible CG, Ford JM, Mathalon DH, Gollub R, Lauriello J, O'Leary D, van Erp TG, Toga AW, Preda A, Lim KO. 2009. Working memory and DLPFC inefficiency in schizophrenia: the FBIRN study. *Schizophrenia bulletin* 35:19-31.
- Raichle ME, MacLeod AM, Snyder AZ, Powers WJ, Gusnard DA, Shulman GL. 2001. A default mode of brain function. *Proceedings of the National Academy of Sciences of the United States of America* 98:676-682.
- Reilly JL, Harris MS, Keshavan MS, Sweeney JA. 2006. Adverse effects of risperidone on spatial working memory in first-episode schizophrenia. *Arch Gen Psychiatry* 63:1189-1197.
- Roebroek A, Formisano E, Goebel R. 2005. Mapping directed influence over the brain using Granger causality and fMRI. *NeuroImage* 25:230-242.
- Sakai K, Rowe JB, Passingham RE. 2002. Active maintenance in prefrontal area 46 creates distractor-resistant memory. *Nature neuroscience* 5:479-484.

- Sass H, Wittchen H. 2003. Diagnostisches und Statistisches Manual Psychischer Störungen. Textrevision.
- Schlosser RG, Koch K, Wagner G, Nenadic I, Roebel M, Schachtzabel C, Axer M, Schultz C, Reichenbach JR, Sauer H. 2008. Inefficient executive cognitive control in schizophrenia is preceded by altered functional activation during information encoding: an fMRI study. *Neuropsychologia* 46:336-347.
- Sehatpour P, Molholm S, Schwartz TH, Mahoney JR, Mehta AD, Javitt DC, Stanton PK, Foxe JJ. 2008. A human intracranial study of long-range oscillatory coherence across a frontal-occipital-hippocampal brain network during visual object processing. *Proceedings of the National Academy of Sciences of the United States of America* 105:4399-4404.
- Silver H, Feldman P, Bilker W, Gur RC. 2003. Working memory deficit as a core neuropsychological dysfunction in schizophrenia. *Am J Psychiatry* 160:1809-1816.
- Stephane M, Pellizzer G. 2007. The dynamic architecture of working memory in schizophrenia. *Schizophrenia research* 92:160-167.
- Tan HY, Callicott JH, Weinberger DR. 2007. Dysfunctional and compensatory prefrontal cortical systems, genes and the pathogenesis of schizophrenia. *Cereb Cortex* 17 Suppl 1:i171-181.
- Tan HY, Sust S, Buckholtz JW, Mattay VS, Meyer-Lindenberg A, Egan MF, Weinberger DR, Callicott JH. 2006. Dysfunctional prefrontal regional specialization and compensation in schizophrenia. *Am J Psychiatry* 163:1969-1977.
- Tek C, Gold J, Blaxton T, Wilk C, McMahon RP, Buchanan RW. 2002. Visual perceptual and working memory impairments in schizophrenia. *Arch Gen Psychiatry* 59:146-153.
- Thormodsen R, Jensen J, Holmen A, Juuhl-Langseth M, Emblem KE, Andreassen OA, Rund BR. 2011. Prefrontal hyperactivation during a working memory task in early-onset schizophrenia spectrum disorders: an fMRI study. *Psychiatry research* 194:257-262.
- Ungerleider LG, Courtney SM, Haxby JV. 1998. A neural system for human visual working memory. *Proceedings of the National Academy of Sciences of the United States of America* 95:883-890.
- White T, Hongwanishkul D, Schmidt M. 2011a. Increased anterior cingulate and temporal lobe activity during visuospatial working memory in children and adolescents with schizophrenia. *Schizophrenia research* 125:118-128.
- White T, Schmidt M, Kim DI, Calhoun VD. 2011b. Disrupted functional brain connectivity during verbal working memory in children and adolescents with schizophrenia. *Cereb Cortex* 21:510-518.
- Whitfield-Gabrieli S, Thermenos HW, Milanovic S, Tsuang MT, Faraone SV, McCarley RW, Shenton ME, Green AI, Nieto-Castanon A, LaViolette P, Wojcik J, Gabrieli JD, Seidman LJ. 2009. Hyperactivity and hyperconnectivity of the default network in schizophrenia and in first-degree relatives of persons with schizophrenia. *Proceedings of the National Academy of Sciences of the United States of America* 106:1279-1284.
- Winterer G, Weinberger DR. 2004. Genes, dopamine and cortical signal-to-noise ratio in schizophrenia. *Trends in neurosciences* 27:683-690.

Table 1. Demographic and clinical characteristics

Variable	Patients (n=17)	Controls (n=17)	P Value
Age (range)	17.9 (15.2–20.4)	17.5 (15.1–19.9)	$t_{(32)}=0.87$, $p=.48$
Sex (male/female)	11 / 6	11 / 6	$\chi^2 (1)=0$, $p<.99$
Handedness (right/left)	13 / 4	13 / 4	$\chi^2 (1)=0$, $p<.99$
Mean Premorbid IQ	96 (SD 16)	97 (9)	$t_{(32)}=-0.21$, $p=.83$
Years of Illness	1.4 (SD 0.9)		
Age at Onset	16.5 (SD 1.2)		
Mean PANSS Score	44.92 (SD 18.38)		
Antipsychotic medication			
Quetiapine	10		
Risperidone	2		
Clozapine	1		
Olanzapine	1		
Aripiprazole	2		
Perphenazine	1		
Mean (SD) Chlorpromazine Equivalents, mg/d	188.7 (166.0)		

Table 2. ANOVA results encoding

Map Index		Name	BA	No of Vertices	Talairach coordinates			WM Load 1	WM Load 2	WM Load 3
					x	y	z	$t_{(32)}$	$t_{(32)}$	$t_{(32)}$
1	left	VLPFC	45	56	-48	25	12	2.91 ^c	2.88 ^c	3.79 ^c
2	left	IPL	40	126	-54	-43	26	2.55 ^b	3.61 ^c	4.52 ^c
3	left	VLFPFC	44	97	-48	11	12	0.32	2.75 ^c	3.71 ^c
4	left	insula	13	79	-34	4	6	-2.15 ^b	0.51	2.99 ^c
5	left	middle temporal gyrus	37	197	-50	-55	7	-1.21	2.06 ^b	3.12 ^c
6	left	precuneus	31	195	-6	-68	27	-1.63	1.90 ^a	2.85 ^c
7	right	lingual gyrus	18	181	18	-56	4	-2.41 ^b	2.06 ^b	1.92 ^a
8	right	IPL	40	101	57	-41	26	2.12 ^b	1.79 ^a	2.05 ^b

^a $p < .1$ (trend) ^b $p < .05$ ^c $p < .01$

Table 3. ANOVA results early maintenance

Map Index		Name	BA	No of Vertices	Talairach coordinates			WM Load 1	WM Load 2	WM Load 3
					x	y	z	$t_{(32)}$	$t_{(32)}$	$t_{(32)}$
1	left	insula	13	418	-40	-26	17	2.94 ^c	3.14 ^c	3.86 ^c
2	left	middle temporal gyrus	19	83	-45	-63	13	1.11	2.31 ^b	3.49 ^c
3	left	middle occipital gyrus	19	79	-24	-81	14	3.15 ^c	3.80 ^c	3.63 ^c
4	left	precuneus	31	240	-5	-68	23	3.39 ^c	4.45 ^c	3.75 ^c
5	left	posterior cingulate cortex	31	230	-10	-33	38	2.64 ^b	4.28 ^c	3.20 ^c
6	right	central sulcus	1,2	125	19	-32	58	2.68 ^b	3.64 ^c	2.55 ^b
7	right	supramarginal gyrus	40	286	51	-25	24	2.46 ^b	3.63 ^c	3.95 ^c
8	right	superior temporal gyrus	41	152	51	-29	16	2.92 ^c	2.61 ^b	3.56 ^c
9	right	middle occipital gyrus	19	116	24	-80	16	3.88 ^c	3.84 ^c	4.83 ^c
10	right	posterior cingulate cortex	31	134	12	-30	41	2.07 ^b	3.95 ^c	2.28 ^b
11	right	precuneus	31	187	7	-65	25	2.42 ^b	4.58 ^c	3.41 ^c
12	right	lingual gyrus	18	78	8	-76	-11	2.12 ^b	4.60 ^c	4.11 ^c
13	left	DLFPC	9	47	-37	10	38	-1.98 ^a	1.58	3.47 ^c
14	left	FEF	6, 9	48	-26	-12	51	-1.84 ^a	-1.53	1.86 ^a
15	left	SPL	7	126	-31	-50	44	-1.47	-1.70 ^a	1.59
16	left	posterior IPS	19	131	-30	-62	37	-0.29	-2.56 ^b	2.05 ^b
17	left	posterior IPS	7	96	-23	-67	35	-0.05	-0.37	2.68 ^b
18	right	SPL	7	107	31	-49	42	-0.14	-0.79	2.75 ^c

^ap<.1 (trend)^bp<.05^cp<.01

Table 4. ANOVA results late maintenance

Map Index	Name	BA	No of Vertices	Talairach coordinates			WM Load 1	WM Load 2	WM Load 3
				x	y	z	$t_{(32)}$	$t_{(32)}$	$t_{(32)}$
1	left superior frontal gyrus	6	83	-16	-14	62	-3.01 ^c	-2.18 ^b	-3.25 ^c
2	left superior temporal gyrus	39	185	-45	-54	20	1.61	3.58 ^c	2.22 ^b
3	left posterior cingulate cortex	31	63	-5	-41	29	1.18	4.14 ^c	1.91 ^a

^a $p < .1$ (trend) ^b $p < .05$ ^c $p < .01$

Table 5. ANOVA results retrieval

Map Index		Name	BA	No of Vertices	Talairach coordinates			WM Load 1	WM Load 2	WM Load 3
					x	y	z	$t_{(32)}$	$t_{(32)}$	$t_{(32)}$
1	left	anterior PFC	10	31	-33	48	18	-1.72 ^a	-3.74 ^c	-2.70 ^b
2	left	inferior VLPFC	47	37	-27	20	-3	-1.65	-2.80 ^c	-3.19 ^c
3	left	IPL	2, 40	94	-49	-25	35	-4.12 ^c	-2.72 ^b	-3.17 ^c
4	left	IPL	40	36	-37	-48	37	-2.73 ^b	-2.80 ^c	-2.40 ^b
5	left	anterior cingulate gyrus	32	19	-8	27	26	-1.18	-3.61 ^c	-2.56 ^b
6	right	inferior VLPFC	47	36	28	19	2	-1.92 ^a	-3.02 ^c	-2.29 ^b
7	right	IPL	2, 40	50	38	-30	41	-2.62 ^b	-3.39 ^c	-2.92 ^c
8	right	lingual gyrus	18	16	11	-86	-7	-1.35	-3.85 ^c	-2.48 ^b
9	left	fusiform gyrus	37	88	-30	-38	-11	2.62 ^b	-1.40	0.77
10	right	anterior cingulate gyrus	32	47	5	22	28	2.04 ^b	-2.79 ^c	-1.73 ^a

^ap<.1 (trend) ^bp<.05 ^cp<.01

Figure Legends

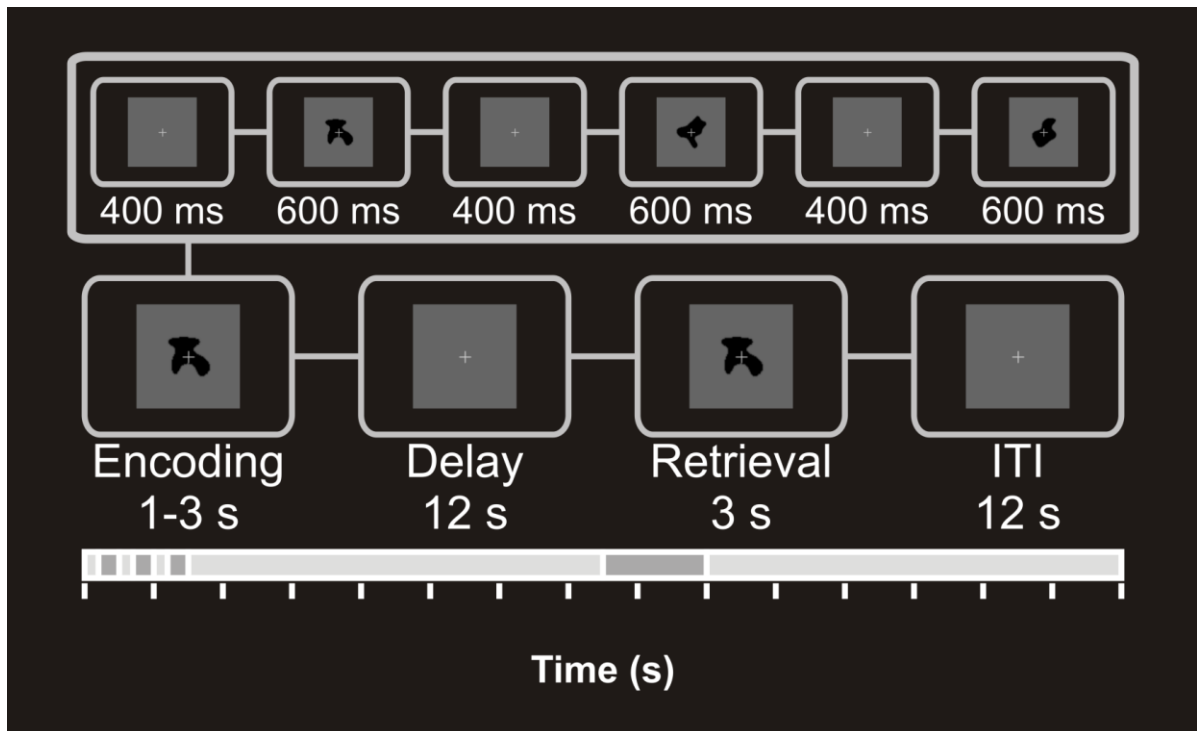


Figure 1. Working memory paradigm.

The delayed discrimination task with random shapes. Memory load was varied by presenting one to three objects for encoding for 600 msec each with an interstimulus interval of 400 msec. After a 12 second delay interval a probe stimulus was presented for 3 seconds. Subjects had to judge whether or not it was part of the initial sample set by pressing a button. The intertrial interval was 12 seconds.

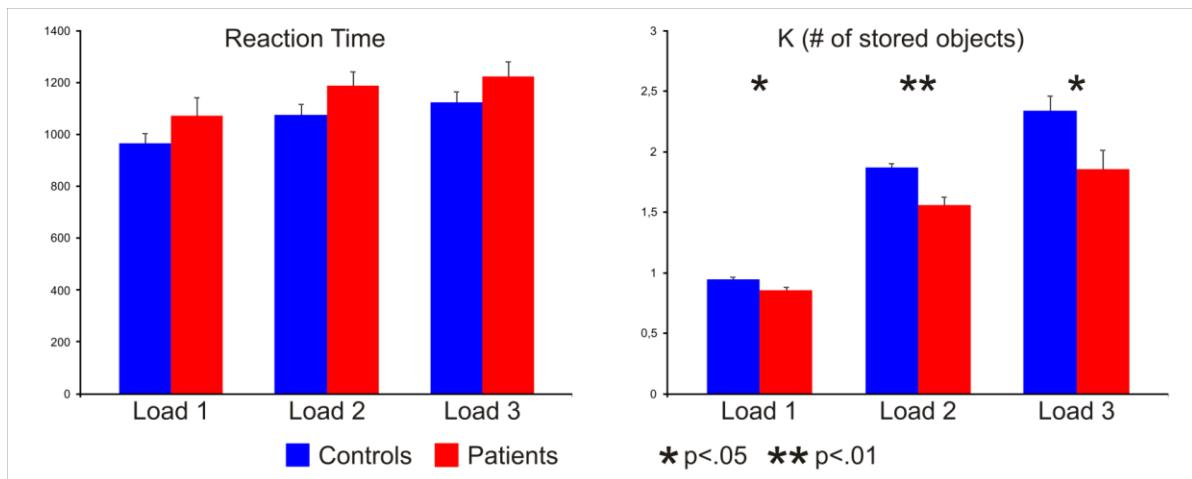


Figure 2. Behavioral parameters.

Mean reaction time (left) and mean K (the number of objects stored in WM) (right) for each memory load condition are shown for controls (blue) and patients (red). Error bars represent SEM. * $p < .05$, ** $p < .01$.

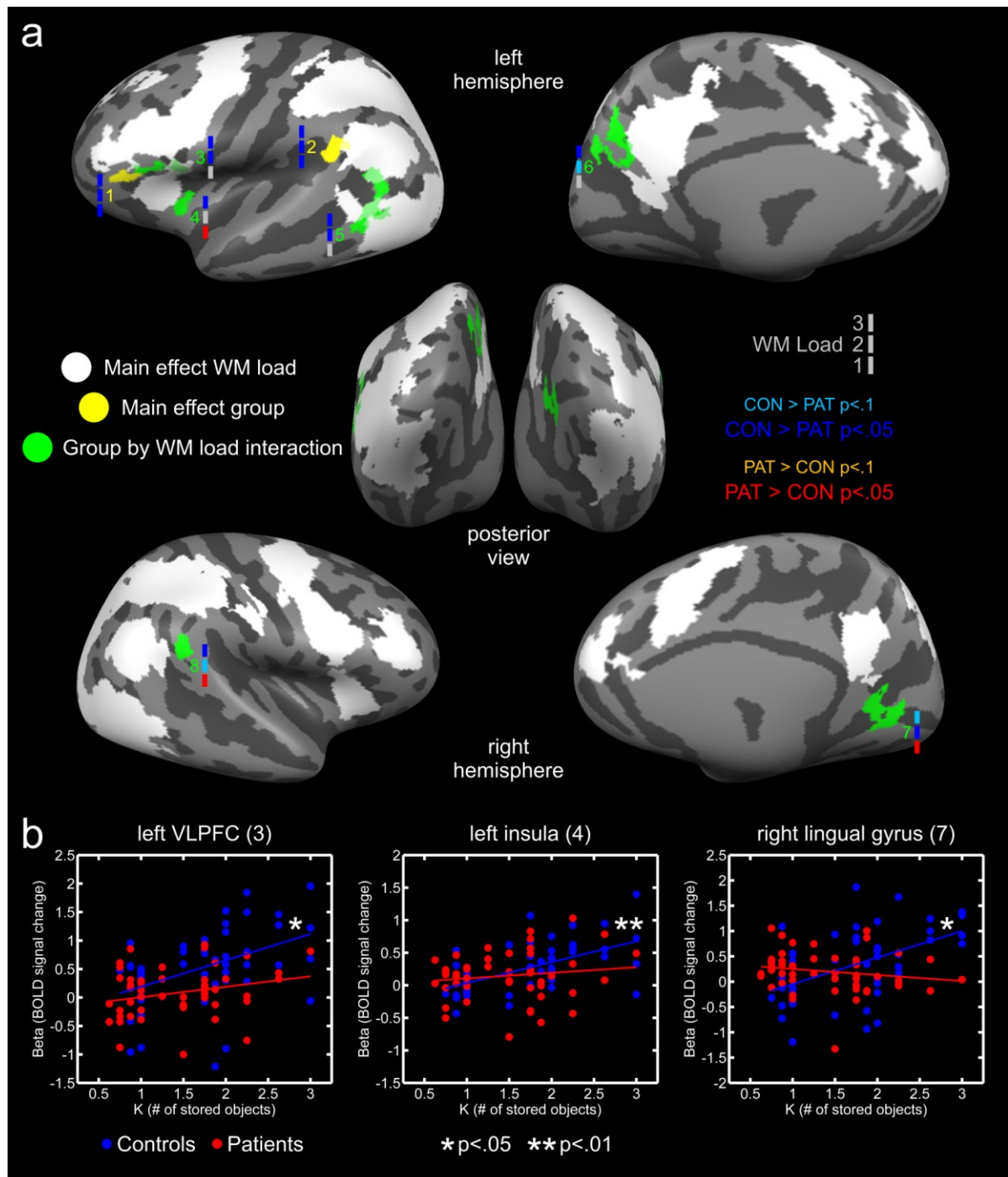


Figure 3. ANOVA results encoding.

a) F-maps of the ANOVA for encoding ($p < .05$, corrected using cluster thresholding). Areas, which showed a main effect of memory load (CLT 142 mm²), are depicted in white. Areas, which showed a main effect of group (CLT 37 mm²), are depicted in yellow. Areas, which showed a group by memory load interaction (CLT 52 mm²), are depicted in green.

The numbers next to each area showing either a main effect of group or a group by memory load interaction correspond to the respective indices in Table 2.

Additionally, next to each index number the results of the two-tailed t-tests for group differences for each memory load condition are represented by three colored vertical bars. The lower bar corresponds to the memory load 1, the middle bar corresponds to the memory load 2 and the upper bar corresponds to the memory load 3 condition. For these bars, blue indicates significantly higher activation ($p < 0.05$) in controls compared to patients, while light blue indicates a trend ($p < 0.1$). Red indicates significantly higher activation ($p < 0.05$) in patients compared to controls, while orange indicates a trend ($p < 0.1$). b) Correlation between BOLD activity and the number of objects stored in WM across all memory load conditions for controls (blue) and patients (red). * $p < .05$, ** $p < .01$. VLPFC: ventrolateral prefrontal cortex.

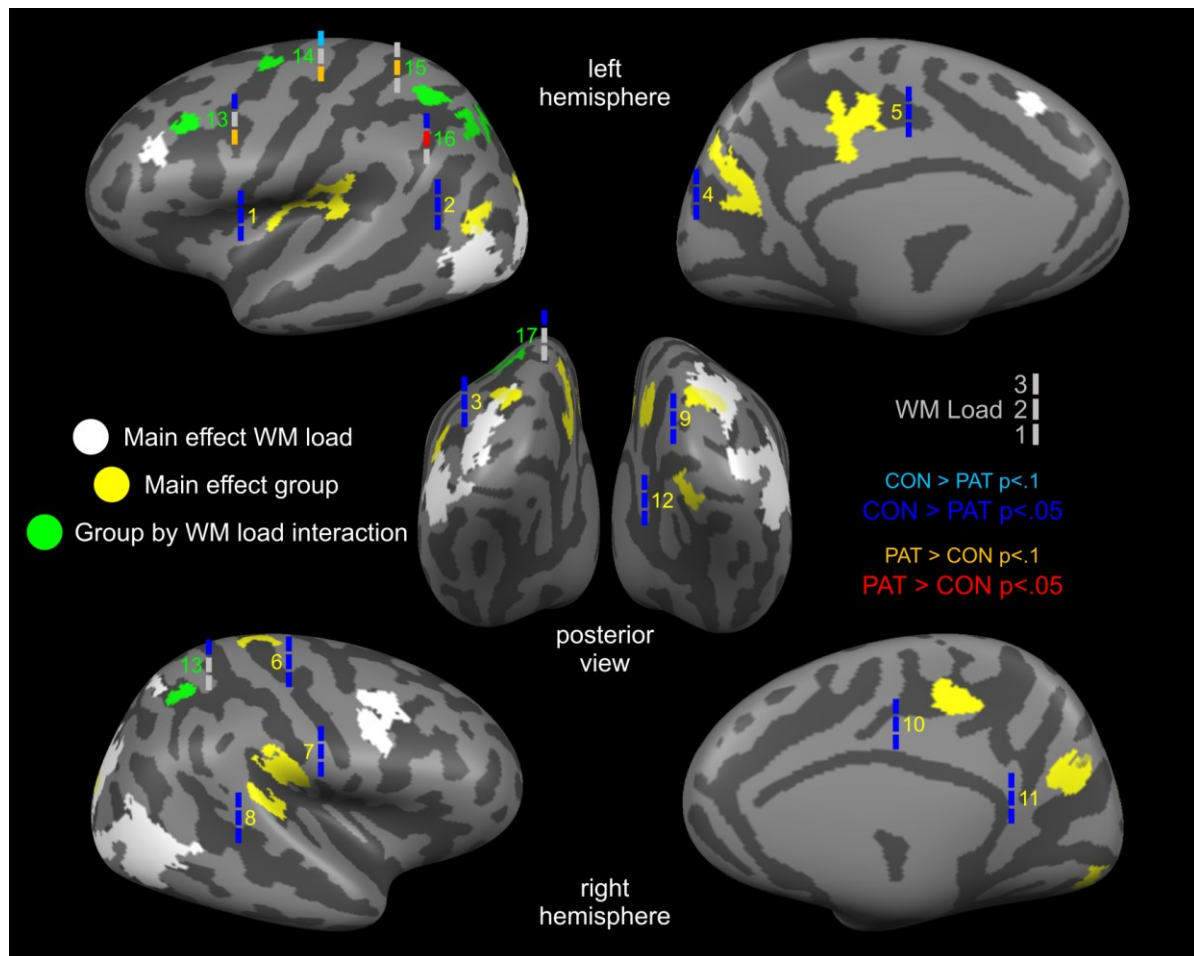


Figure 4. ANOVA results early maintenance.

F-maps of the ANOVA for early maintenance ($p < .05$, corrected using cluster thresholding). Areas, which showed a main effect of memory load (CLT 64 mm^2), are depicted in white. Areas, which showed a main effect of group (CLT 61 mm^2), are depicted in yellow. Areas, which showed a group by memory load interaction (CLT 33 mm^2), are depicted in green. The numbers next to each area with a main effect of group or a group by memory load interaction correspond to the respective indices in Table 3. Additionally, next to each index number the results of the two-tailed t-tests for group differences for each memory load condition are represented by three colored vertical bars. The lower bar corresponds to the memory load 1, the middle bar corresponds to the memory load 2 and the upper bar corresponds to the memory load 3 condition. For these bars, blue indicates significantly higher

activation ($p < 0.05$) in controls compared to patients, while light blue indicates a trend ($p < 0.1$). Red indicates significantly higher activation ($p < 0.05$) in patients compared to controls, while orange indicates a trend ($p < 0.1$).

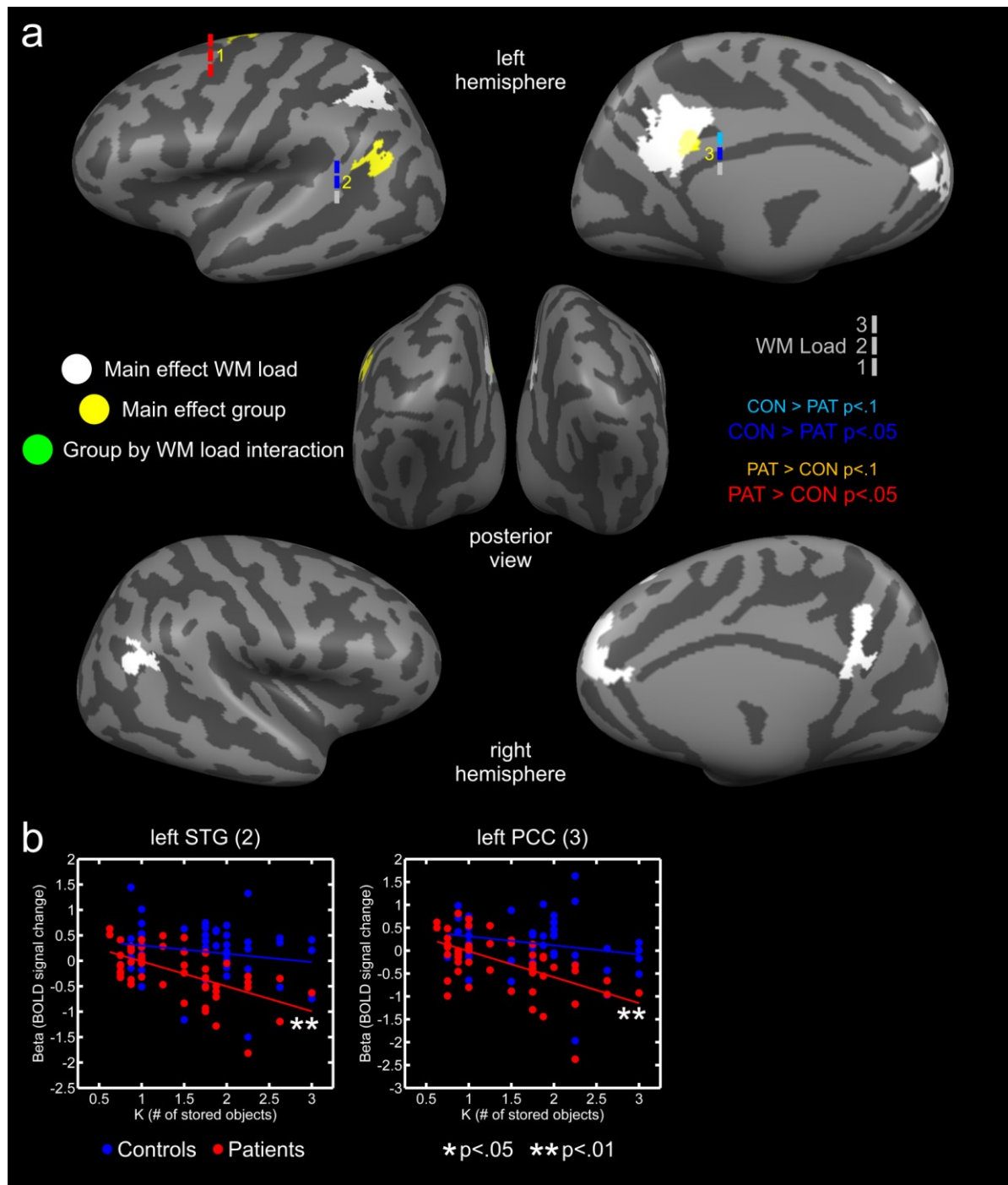


Figure 5. ANOVA results late maintenance.

a) F-maps of the ANOVA for late maintenance ($p < .05$, corrected using cluster thresholding). Areas, which showed a main effect of memory load (CLT 72 mm²), are depicted in white. Areas, which showed a main effect of group (CLT 37 mm²), are depicted in yellow. No area showed a significant group by memory load interaction. The numbers next to each area showing a main effect of group

correspond to the respective indices in Table 4. Additionally, next to each index number the results of the two-tailed t-tests for group differences for each memory load condition are represented by three colored vertical bars. The lower bar corresponds to the memory load 1, the middle bar corresponds to the memory load 2 and the upper bar corresponds to the memory load 3 condition. For these bars, blue indicates significantly higher activation ($p < 0.05$) in controls compared to patients, while light blue indicates a trend ($p < 0.1$). Red indicates significantly higher activation ($p < 0.05$) in patients compared to controls, while orange indicates a trend ($p < 0.1$). b) Correlation between BOLD activity and the number of objects stored in WM across all memory load conditions for controls (blue) and patients (red). * $p < .05$, ** $p < .01$. STG: superior temporal gyrus, PCC: posterior cingulate cortex.

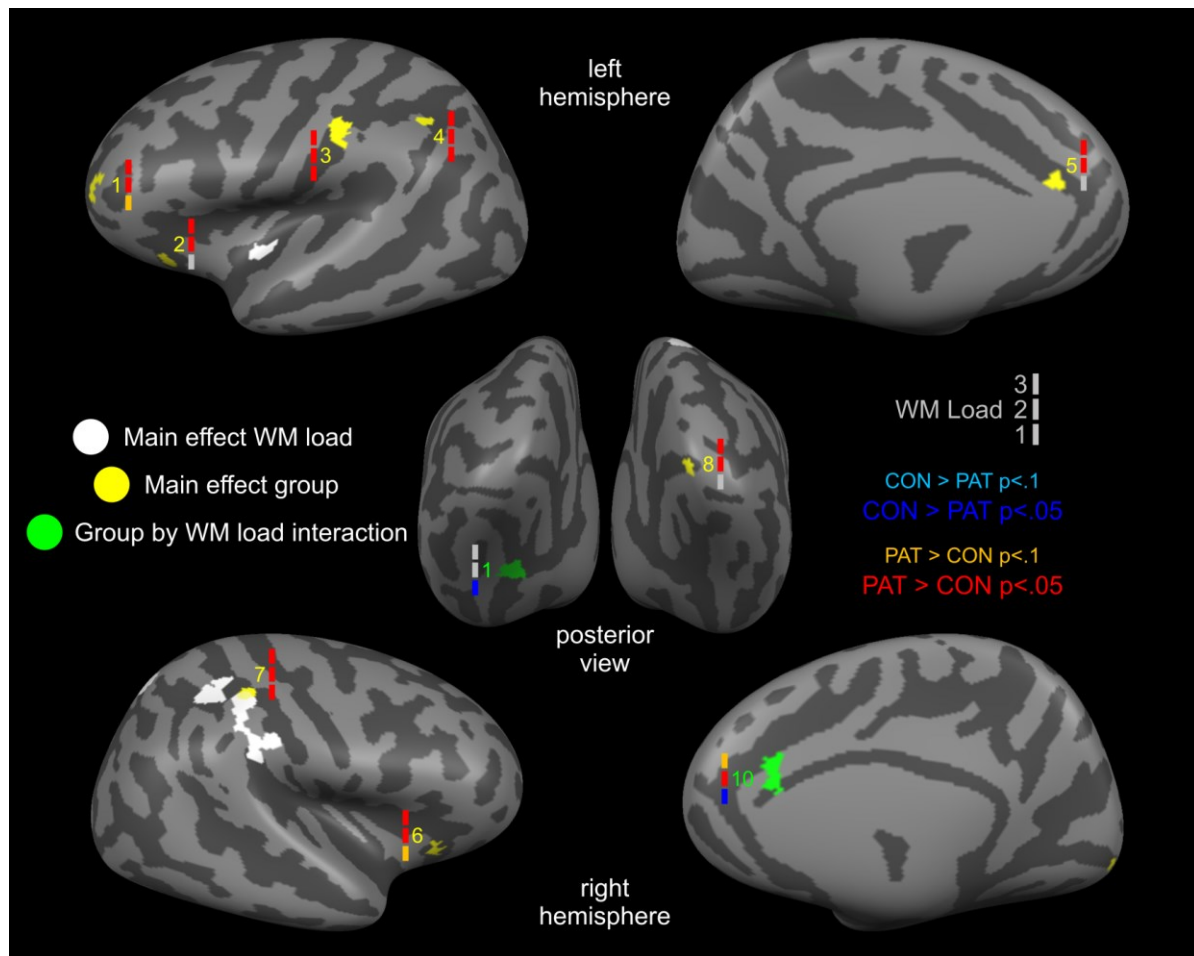


Figure 6. ANOVA results retrieval.

F-maps of the ANOVA for retrieval ($p < .05$, corrected using cluster thresholding). Areas, which showed a main effect of memory load (CLT 47 mm²), are depicted in white. Areas, which showed a main effect of group (CLT 15 mm²), are depicted in yellow. Areas, which showed a group by memory load interaction (CLT 37 mm²), are depicted in green. The numbers next to each area showing either a main effect of group or a group by memory load interaction correspond to the respective indices in Table 5. Additionally, next to each index number the results of the two-tailed t-tests for group differences for each memory load condition are represented by three colored vertical bars. The lower bar corresponds to the memory load 1, the middle bar corresponds to the memory load 2 and the upper bar corresponds to the memory load 3 condition. For these bars, blue indicates significantly higher

activation ($p < 0.05$) in controls compared to patients, while light blue indicates a trend ($p < 0.1$). Red indicates significantly higher activation ($p < 0.05$) in patients compared to controls, while orange indicates a trend ($p < 0.1$).

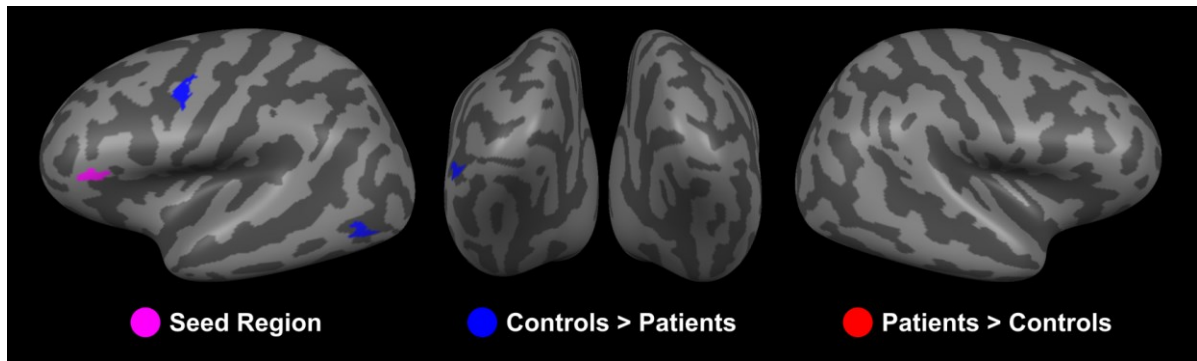


Figure 7. Functional connectivity results encoding.

t-map depicting significant group differences in the strength of functional connectivity during encoding for the left VLPFC (two-tailed t-tests, random effects level, $p < .05$, corrected using cluster thresholding; CLT 45 mm^2). Blue areas indicate stronger connectivity with the seed region for controls, red areas indicate stronger connectivity with the seed region for patients (two-tailed t-tests, random effects level).

Supplementary Material

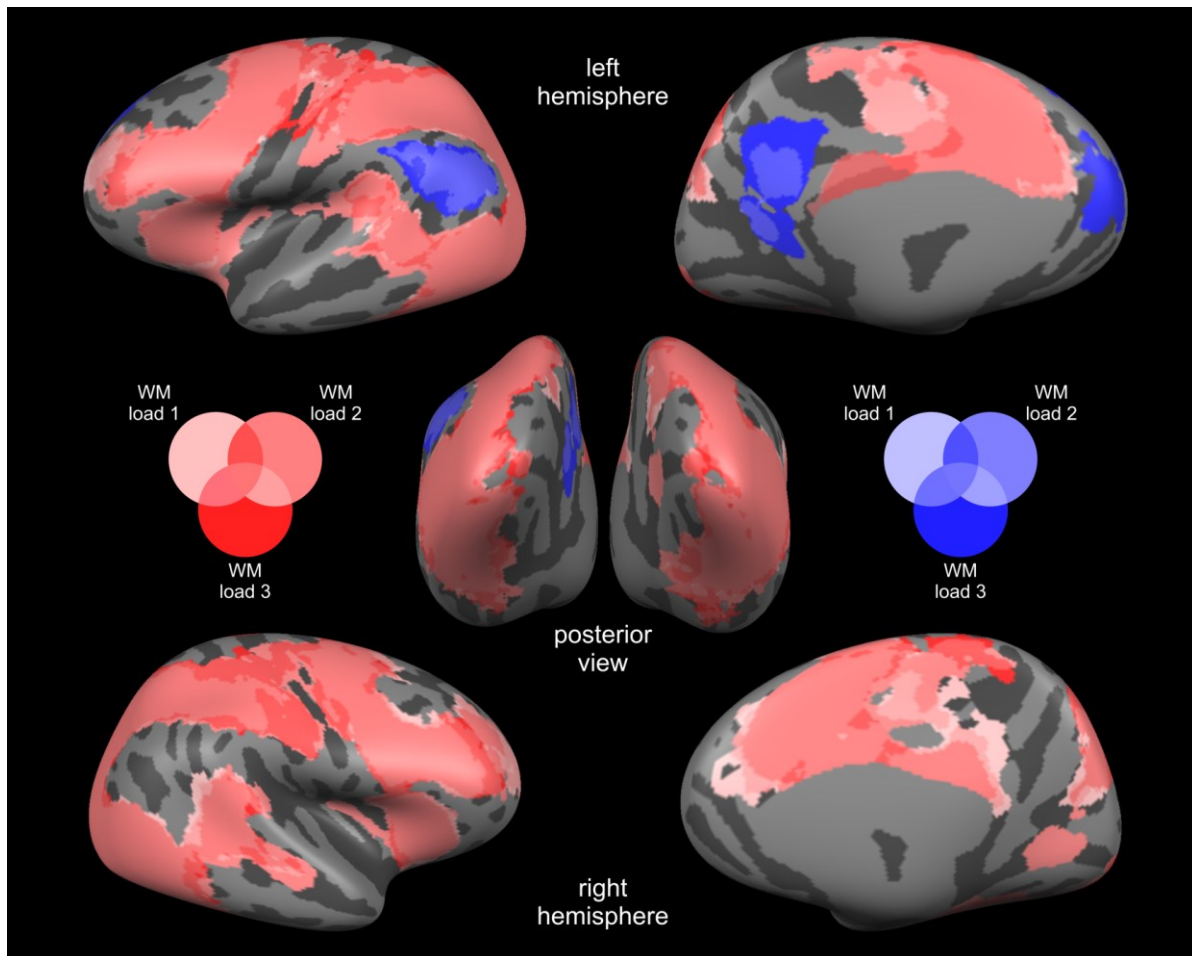


Figure S1. Task-related activation and deactivation maps encoding.

Superimposition maps showing the cortical networks engaged in both patients and controls during encoding for each WM load condition (t-test, $p < .05$, corrected using cluster thresholding). Areas showing task related activation are depicted in red, areas showing task related deactivation are depicted in blue. Each WM load condition is associated with an increasingly darker shade of red and blue, reflecting increasing WM load. Colors are superimposed and areas of overlap (cortical regions showing activation or deactivation during more than one WM load condition) receive the appropriate mixed color.

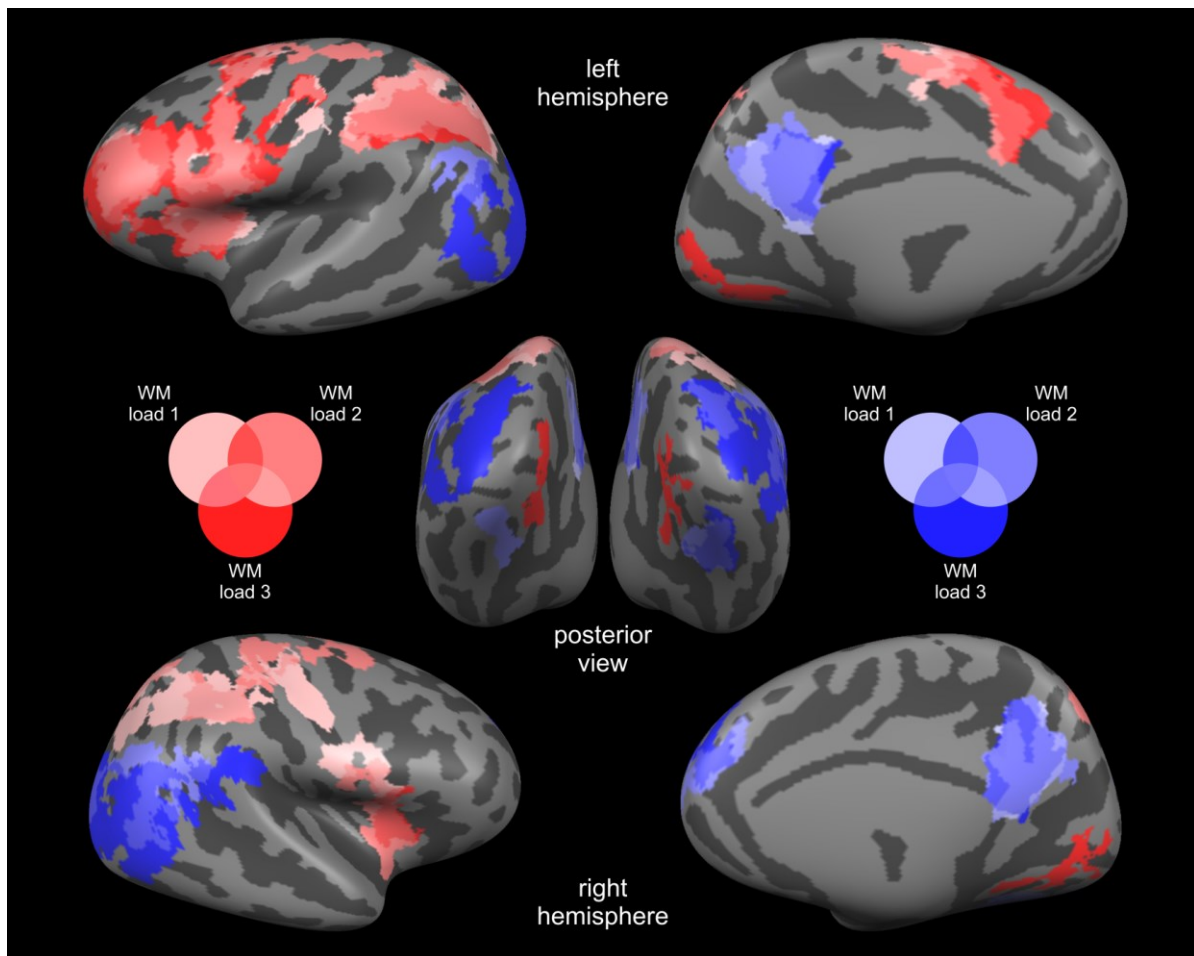


Figure S2. Task-related activation and deactivation maps early maintenance.

Superimposition maps showing the cortical networks engaged in both patients and controls during early maintenance for each WM load condition (t-test, $p < .05$, corrected using cluster thresholding). Areas showing task related activation are depicted in red, areas showing task related deactivation are depicted in blue. Each WM load condition is associated with an increasingly darker shade of red and blue, reflecting increasing WM load. Colors are superimposed and areas of overlap (cortical regions showing activation or deactivation during more than one WM load condition) receive the appropriate mixed color.

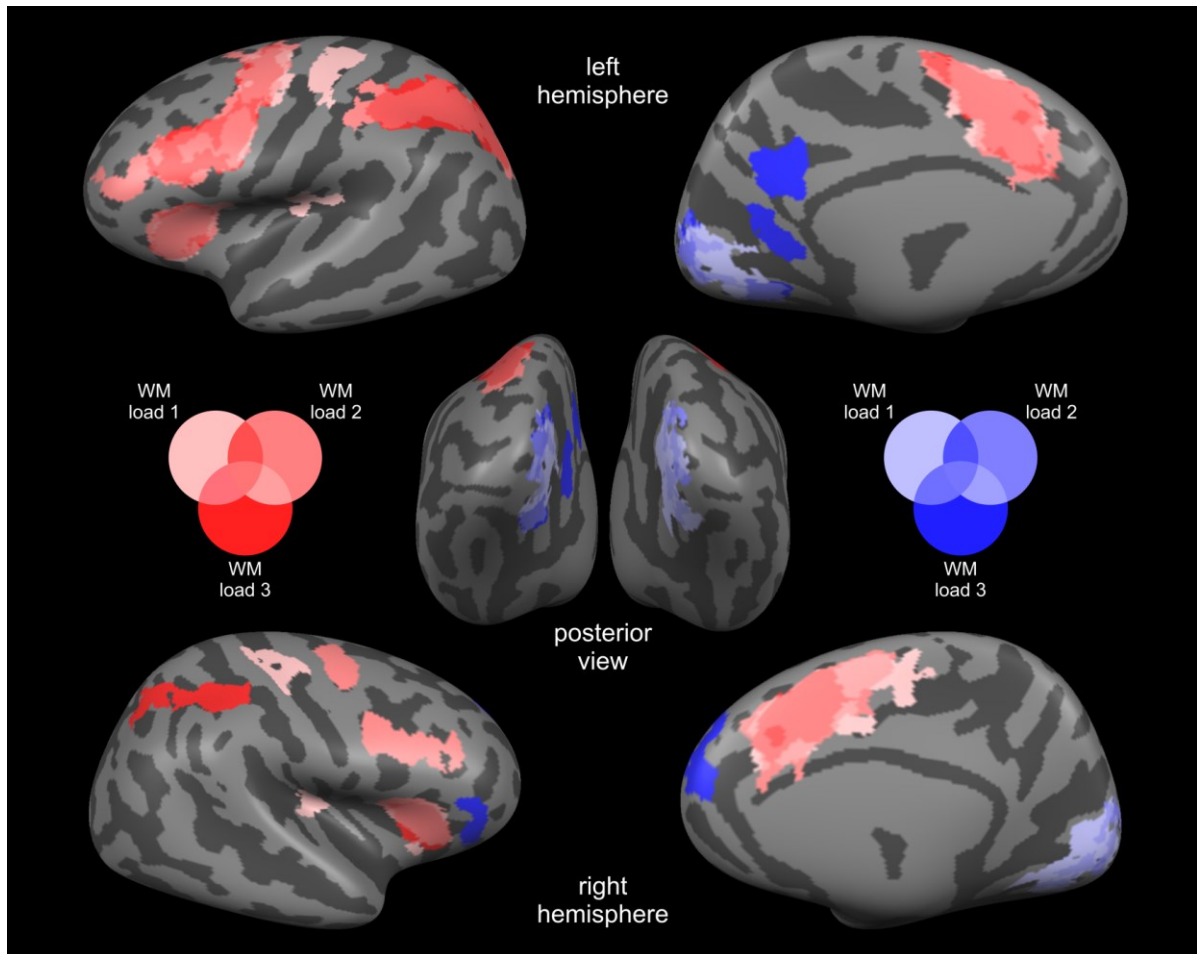


Figure S3. Task-related activation and deactivation maps late maintenance.

Superimposition maps showing the cortical networks engaged in both patients and controls during late maintenance for each WM load condition (t-test, $p < .05$, corrected using cluster thresholding). Areas showing task related activation are depicted in red, areas showing task related deactivation are depicted in blue. Each WM load condition is associated with an increasingly darker shade of red and blue, reflecting increasing WM load. Colors are superimposed and areas of overlap (cortical regions showing activation or deactivation during more than one WM load condition) receive the appropriate mixed color.

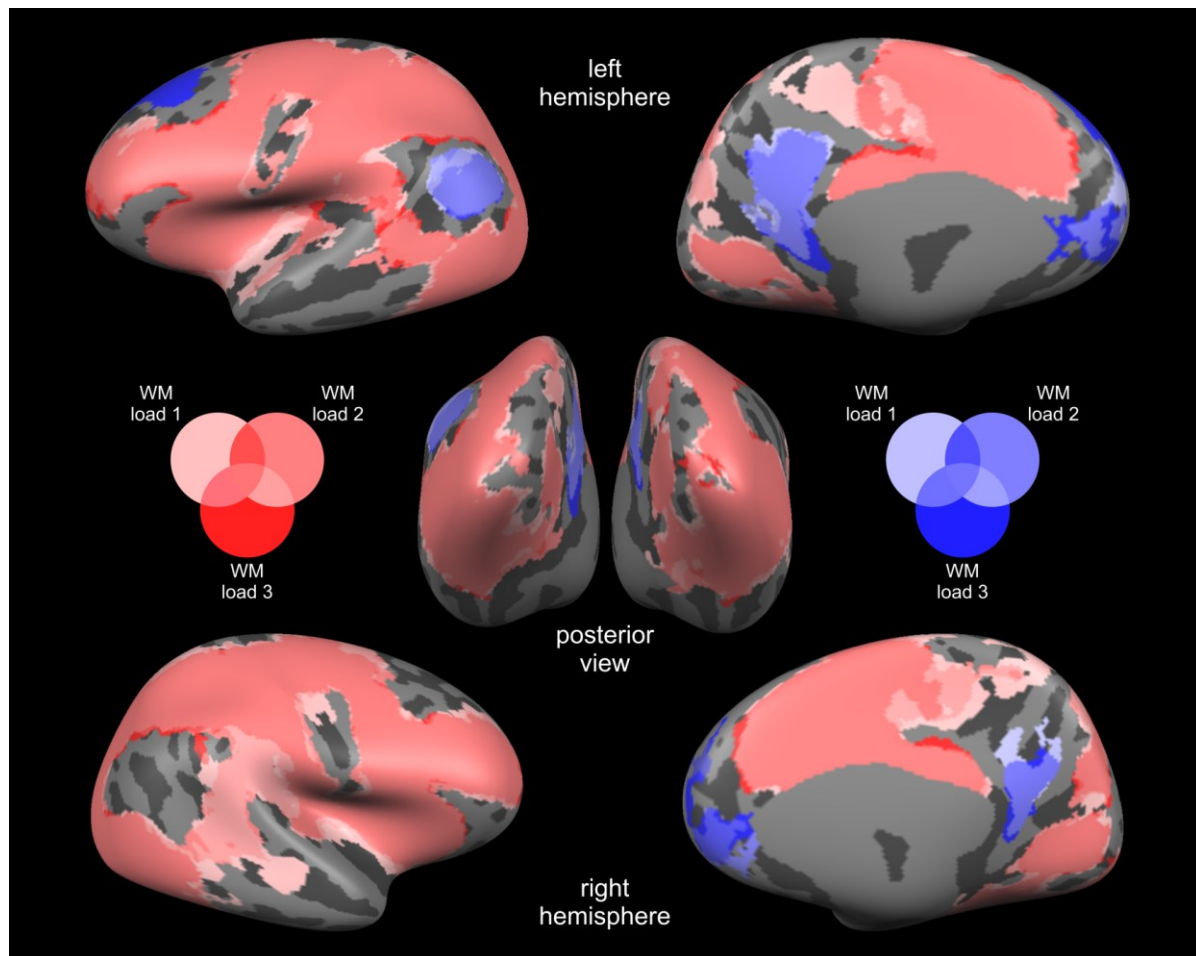


Figure S4. Task-related activation and deactivation maps retrieval.

Superimposition maps showing the cortical networks engaged in both patients and controls during retrieval for each WM load condition (t-test, $p < .05$, corrected using cluster thresholding). Areas showing task related activation are depicted in red, areas showing task related deactivation are depicted in blue. Each WM load condition is associated with an increasingly darker shade of red and blue, reflecting increasing WM load. Colors are superimposed and areas of overlap (cortical regions showing activation or deactivation during more than one WM load condition) receive the appropriate mixed color.

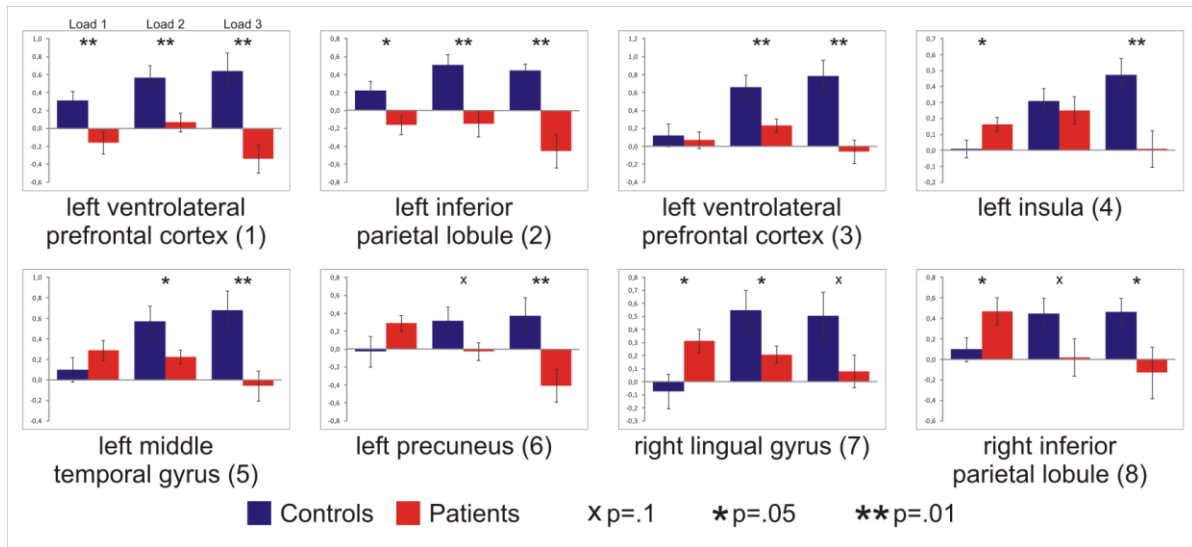


Figure S5. Beta values encoding.

Beta values for the regions of interest derived from the ANOVA for encoding for controls (blue) and patients (red). The number for each region corresponds to its index in Figure 3 and Table 2. Error bars represent SEM.

X p<.1, *p<.05, **p<.01.

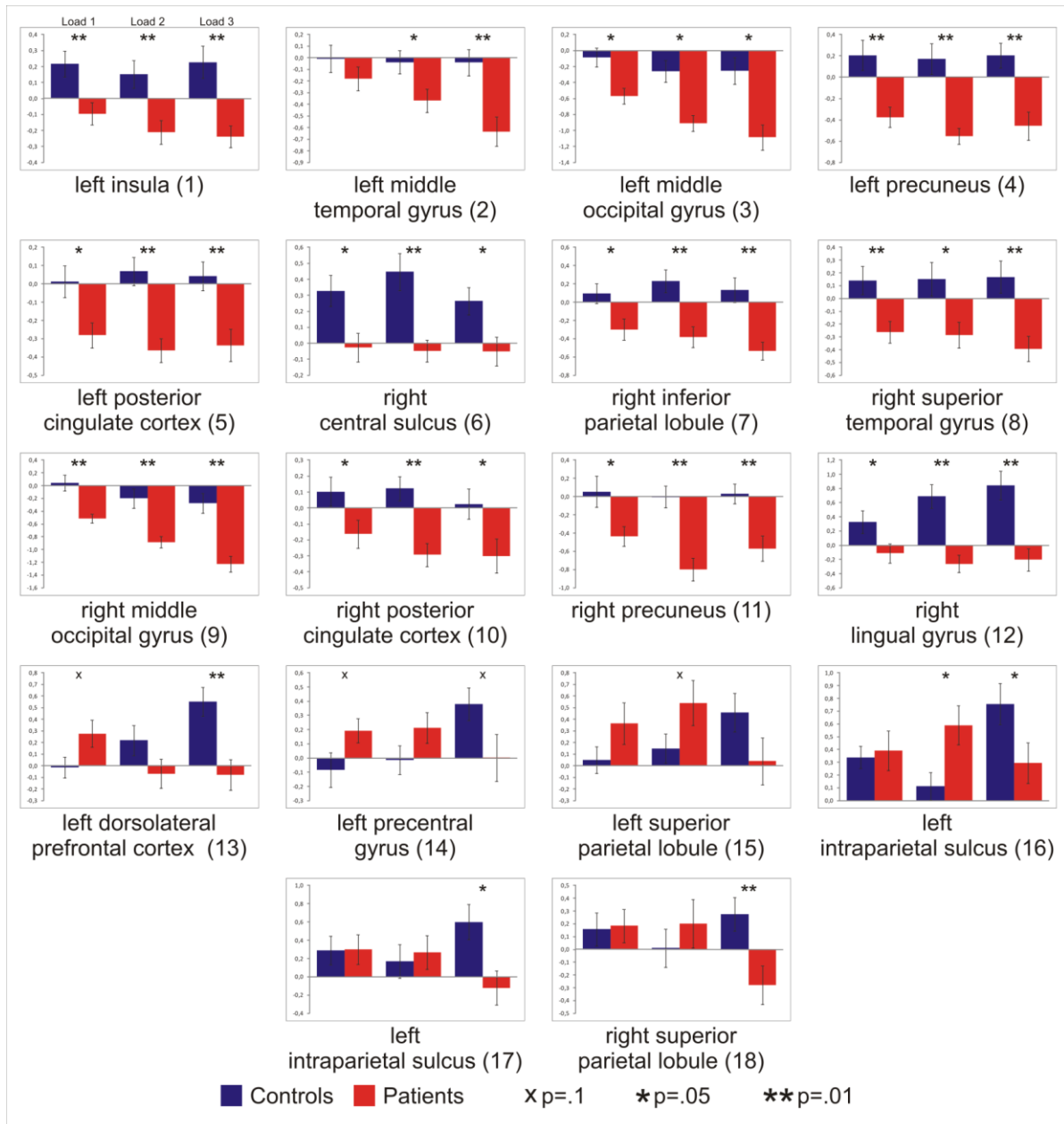


Figure S6. Beta values early maintenance.

Beta values for the regions of interest derived from the ANOVA for early maintenance for controls (blue) and patients (red). The number for each region corresponds to its index in Figure 4 and Table 3. Error bars represent SEM.

^xp<.1, *p<.05, **p<.01.

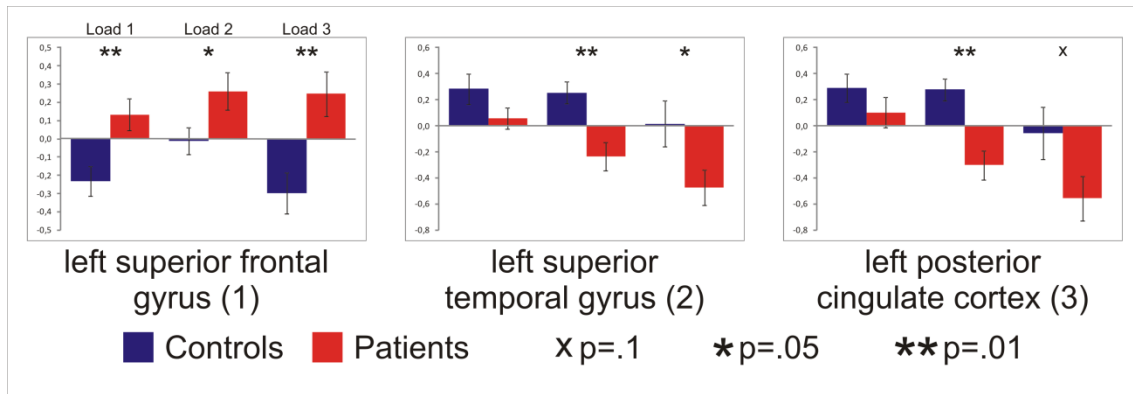


Figure S7. Beta values late maintenance.

Beta values for the regions of interest derived from the ANOVA for late maintenance for controls (blue) and patients (red). The number for each region corresponds to its index in Figure 5 and Table 4. Error bars represent SEM.

X p < .1, * p < .05, ** p < .01.

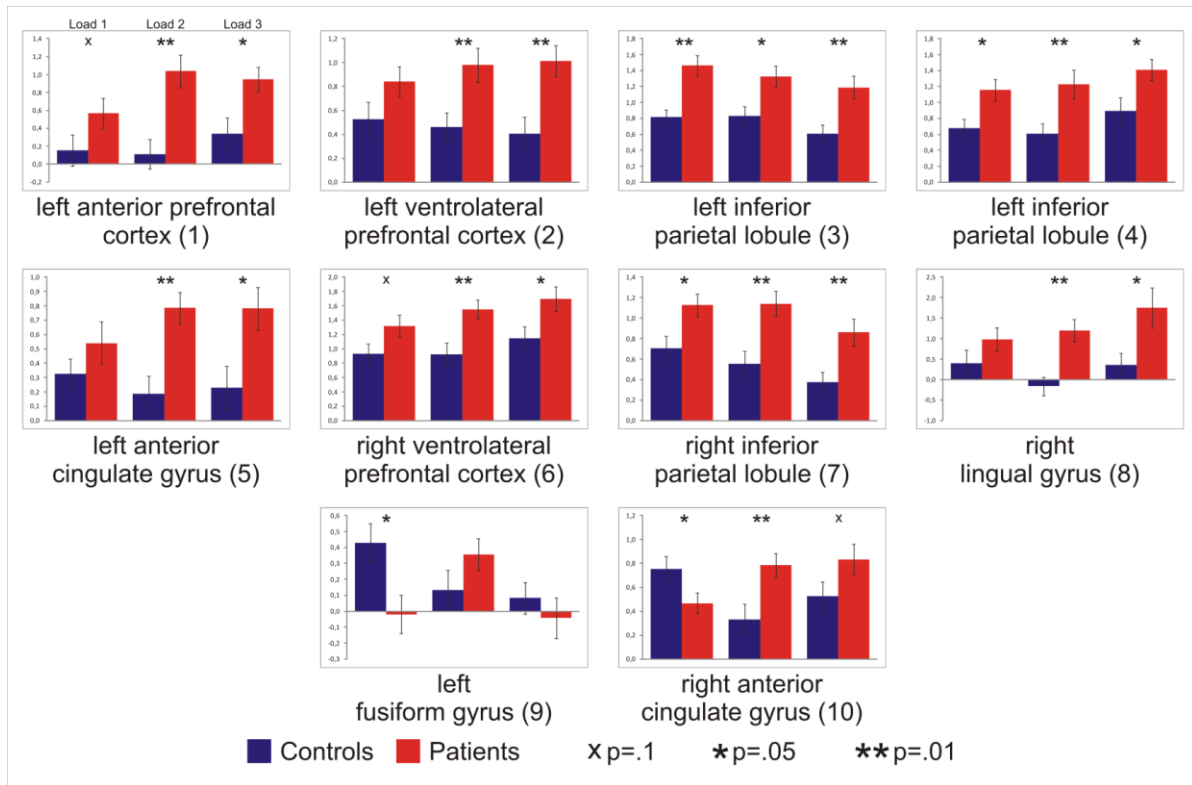


Figure S8. Beta values retrieval. Beta values for the regions of interest derived from the ANOVA for retrieval for controls (blue) and patients (red). The number for each region corresponds to its index in Figure 6 and Table 5. Error bars represent SEM.

X $p < .1$, * $p < .05$, ** $p < .01$.